



Cite this: *Mater. Adv.*, 2023, 4, 6118

## Role of thermal and reactive oxygen species-responsive synthetic hydrogels in localized cancer treatment (bibliometric analysis and review)

Yohannis Wondwosen Ahmed,<sup>a</sup> Hsieh-Chih Tsai,<sup>ID \*abf</sup> Tsung-Yun Wu,<sup>a</sup> Haile Fentahun Darge<sup>a</sup> and Yu-Shuan Chen<sup>\*cde</sup>

Cancer is a major pharmaceutical challenge that necessitates improved care. Modern anti-cancer drugs require well-designed carriers to deliver and release them at the intended location. Hydrogel delivery systems are efficient and therapeutically beneficial *in situ* anti-cancer drug delivery platforms. Hydrogels exhibit excellent biocompatibility, biodegradation pathways, and minimal immunogenicity. Their stimuli-responsive characteristics, such as thermo-response and reactive oxygen species (ROS)-response, make hydrogels ideal for sustained local drug delivery and controlled drug release. Recently, synthetically manufactured thermal and ROS-responsive smart hydrogels enhance treatment efficacy by minimizing toxicities associated with non-carrier-mediated anti-cancer drug delivery. In this review, we discuss synthetically manufactured thermal (poly(*N*-isopropyl acrylamide) (PNIPAM), Pluronic, and polyethylene glycol (PEG)) and ROS-responsive copolymer hydrogels and their application in local anti-cancer drug delivery. We also addressed an extensive bibliometric analysis of the keyword "hydrogels for cancer treatment" to generate the country, source, documents, and author-based rankings maps.

Received 30th June 2023,  
Accepted 26th October 2023

DOI: 10.1039/d3ma00341h

rsc.li/materials-advances

## 1. Introduction

Cancer occurs due to genetic or epigenetic dysregulation, causing uncontrolled growth of malignant cells that invade other body parts.<sup>1</sup> This nature makes cancer the top cause of death globally, with nearly 10 million deaths in 2020 and a projected 13.1 million deaths in 2030.<sup>2-6</sup> In 2022, it was projected that China and USA would experience 3 210 000 and 640 000 cancer-related deaths, respectively.<sup>7</sup> Despite efforts to address complications from unsuccessful treatments, a comprehensive cancer cure remains elusive, barring certain promising results.<sup>8-11</sup> Late-stage frontline treatment options for cancer encompass surgery,<sup>12,13</sup> chemotherapy,<sup>14,15</sup> radiotherapy,<sup>16,17</sup> immunotherapy,<sup>18,19</sup> theragnostic (diagnosis and therapeutics

combined)<sup>20,21</sup> and gene therapy.<sup>22,23</sup> Conventional delivery methods for these treatments demand high dosages to achieve therapeutic effects, potentially leading to toxicity and decreased patient compliance.<sup>24,25</sup> According to recent studies, traditional chemotherapy has contributed to low therapeutic indices, multiple drug resistance, poor absorption, and nonspecific targeting.<sup>6,26</sup> For instance, preoperative and postoperative neoadjuvant chemotherapy with doxorubicin (DOX) and anthracycline, lacking a delivery mechanism, induces cardiac side effects and adverse reactions in patients with breast cancer.<sup>27</sup> These drawbacks have spurred the development of smart drug delivery systems like hydrogels, nano-vesicles, liposomes, and microneedles for controlled local release.<sup>28,29</sup> Lately, hydrogel delivery systems have gained attention due to their ability to minimize toxic drug effects while demonstrating excellent controlled release and biodegradability.<sup>30</sup> Moreover, stimuli-responsive hydrogels for local cancer drug delivery have enhanced the efficacy of cancer treatment modalities<sup>6,31,32</sup> owing to their body mimicking and extended drug release capacity in the local area of cancer cells.<sup>33-36</sup> Rather than local delivery, stimuli-responsive hydrogels can also be synthesized with surface-decorating molecules like aptamers to target receptors or proteins highly expressed by cancer cells,<sup>37,38</sup> reducing the side effects linked to untargeted systemic delivery.<sup>39-42</sup> Hence, smart hydrogels of synthetic origin are suitable for local drug delivery due to their easily modifiable architecture.<sup>43</sup>

<sup>a</sup> Graduate Institute of Applied Science and Technology, National Taiwan University of Science and Technology, Taipei 106, Taiwan, Republic of China.

E-mail: h.c.tsai@mail.ntust.edu.tw

<sup>b</sup> Advanced Membrane Material Center, National Taiwan University of Science and Technology, Taipei 106, Taiwan, Republic of China

<sup>c</sup> Bio Innovation Center, Buddhist Tzu Chi Medical Foundation, Taiwan, Republic of China. E-mail: yushuanchen@gmail.com

<sup>d</sup> Department of Medical Research, Hualien Tzu Chi Hospital, Buddhist Tzu Chi Medical Foundation, Hualien, Taiwan, Republic of China

<sup>e</sup> Tzu Chi University of Science and Technology, Taiwan, Republic of China

<sup>f</sup> R&D Center for Membrane Technology, Chung Yuan Christian University, Chungli, Taoyuan 320, Taiwan, Republic of China



Therefore, here we examine drug delivery applications of synthetic thermally sensitive (such as PNIPAM, Pluronic, and PEG) and ROS-responsive hydrogels, particularly in cancer



**Yohannis Wondwosen Ahmed**

*University of Science and Technology (Taiwan Tech) in the Department of Graduate Institute of Applied Science and Technology, under the guidance of Professor Hsieh-Chih Tsai and Dr Yu Suhan Chen. His research is centered on the development of thermal-sensitive Pluronic F-127-based hydrogels for localized and controlled delivery of anti-cancer drugs.*



**Tsung-Yun Wu**

*His research interests primarily encompass the fields of chemical engineering and polymer modification. Currently, he is conducting research with a specific focus on the modification of Pluronic F127 for drug delivery applications.*

*Yohannis Wondwosen Ahmed, MSc, is a faculty member at Addis Ababa University, College of Health Sciences, Department of Medical Biochemistry. He served as a lecturer of Medical Biochemistry for medical and health science students. He obtained his BSc degree in Applied Chemistry from Ambo University and earned his MSc degree in Biochemistry from Mysore University in 2010 and 2014, respectively. Since February 2022, he has been pursuing his PhD at the National Taiwan*

*treatment. We chose these two stimuli-responsive hydrogels based on their suitability for use in the body's physiological conditions.<sup>44–46</sup> Furthermore, we aim to focus on synthetic-*



**Hsieh-Chih Tsai**

*Dr Hsieh-Chih Tsai currently serves as a Professor and Chairman at the Graduate Institute of Applied Science and Technology at National Taiwan University of Science and Technology (Taiwan Tech). Additionally, he holds the position of Director at the Advanced Membrane Materials Center at Taiwan Tech. Dr Tsai is recognized for his substantial contributions to the field, having authored more than 160 papers in the synthesis of functional polymers and the fabrication of polymer nanocomposites for applications in drug delivery, biomedical devices, bio-contrast agents, and membrane technology (H-index 32 from Scopus).*



**Haile Fentahun Darge**

*Tech) in the Department of Graduate Institute of Applied Science and Technology. His research work focused on the preparation of polymeric biomaterials (injectable smart hydrogels and nanocarriers, microspheres and microneedles) for controlled drug delivery in cancer treatment, wound dressing, and for 3D cell culturing. From Jan 2021–April 2023, he was working as a project assigned postdoctoral research fellow in Prof. Hsieh-Chih Tsai's lab, Taiwan Tech. Currently, he is a postdoctoral research fellow at Center of Ocular Research and Education (CORE), University of Waterloo and his research work is focusing on developing biomaterials for ocular drug delivery and in vitro eye models using 3D printing technology. He has authored 33+ peer-reviewed research articles in the area of drug delivery for cancer treatment.*



based copolymers due to technological advancements that require a comprehensive understanding of the synthetic materials employed in designing and developing hydrogels for cancer therapy. We also assessed in-depth bibliometric analysis of the term “Hydrogels as drug carriers for cancer treatment” for a variety of purposes. (1) To analyze the frequency and distribution of publication in the area allowing gaining insights into how research in this field has evolved. (2) To map the research landscape by identifying key authors, institutions, and countries contributing to the literature, which allows where expertise lies and potential collaborations. (3) To assess the impact of research by looking at citation counts and the effect of specific papers, understanding which studies have had a significant impact on the field. (4) To identify research gaps in the area that may present opportunities for new studies and (5) to quantify the research outputs regarding hydrogels in cancer treatment.<sup>47</sup>

### 1.1. Properties of hydrogels and their general classification

Hydrogels can be designed using nano-, micro-, and macro-sized structural polymers to effectively deliver medications targeting cancer cells.<sup>33,48,49</sup> Their soft and rubbery nature allows them to align with living tissues. Additionally, hydrogels have an insoluble and highly hydrophilic 3D network of polymers synthesized from natural or synthetic materials, offering high flexibility due to their water content.<sup>50–52</sup> However, the retaining capacity of hydrogels is not limited to water; they can also hold solutions of hydrophilic and hydrophobic drugs.<sup>53–56</sup> The fluid retention capabilities are intricately tied to their swelling and deswelling properties, as illustrated in Fig. 1A.<sup>57,58</sup> Swelling involves the absorption of a liquid through the 3D networks of the hydrogel, loading the material.<sup>59,60</sup> Deswelling, triggered by surrounding physicochemical changes, causes hydrogel shrinkage or network opening, releasing the loaded drug.<sup>55,61</sup> Swelling mechanisms involve a three-step process, including the hydrophilic and hydrophobic components of the hydrogel.<sup>62,63</sup> Primary-bound water forms initially through the hydration of the hydrogel's hydrophilic moiety, followed by secondary-bound water

generation due to the interaction between the hydrophobic moiety and primary-bound water. Unbound water or drug solutions can penetrate the spaces between network meshes, utilizing the osmotic driving force resistance provided by the physical and chemical crosslinks of the networks.<sup>64,65</sup> The crosslinking structure of hydrogels (hydrophobic) is critical in preventing the disintegration of the hydrogel structure during swelling.<sup>65</sup> In the absence of a crosslinker structure, the hydrophilic linear chain structure of the hydrogel dissolves due to its polymer chain and its affinity for water.<sup>65–67</sup> The water solubility of these hydrophilic chains is attributed to the presence of hydrophilic groups containing electronegative elements (N and O) in their structure. Chemical cross linkers create strong links, resulting in a solubility imbalance caused by the elastic retractive force at the crosslinking points in their network. Solubility reaches equilibrium and swelling peaks when retraction and elasticity forces balance.<sup>65</sup> Chemical cross-linking is a versatile method for producing hydrogels with enhanced mechanical strength and stability. This increased strength is a result of covalent bonding initiated by chemical linkers, including photo polymerization and enzyme-mediated crosslinking (Fig. 1B).<sup>68</sup> However, chemical crosslinkers can introduce toxicity associated with hydrogel use.<sup>69</sup> To address this issue, new physical crosslink production methods for hydrogels have been developed, offering reduced toxicity but lower mechanical strength than chemical crosslinkers.<sup>70</sup> Recent physical crosslinking techniques for hydrogels include hydrogen (H) bonding, van der Waals interactions, hydrophobic interactions, ionic interactions,  $\pi$ - $\pi$  stacking, and stereo complexation (Fig. 1B).<sup>71,72</sup> When selecting chemical linkers, using low-molecular-weight crosslinkers with the polymer during synthesis *via* mixing is preferable.<sup>72</sup> Additionally, hydrogels have emerged as leading drug carriers for localized and controlled regional cancer treatments due to their high environmental sensitivity, ionic conductivity, permeability, stimuli-responsive potential, and low immunogenicity.<sup>73,74</sup> Among these properties, hydrogels are particularly effective for controlled drug release because they intelligently respond to environmental changes.<sup>75,76</sup>

Besides their application in drug delivery, hydrogels hold significant potential for use in various biomedical fields, including tissue engineering,<sup>78–80</sup> implantation,<sup>81,82</sup> regeneration,<sup>83–85</sup> wound dressing,<sup>86–88</sup> cartilage filler,<sup>89,90</sup> contact lens manufacturing,<sup>50,91</sup> injectable fillers in minimally invasive surgeries<sup>92</sup> and, the synthesis of artificial blood vessels.<sup>93,94</sup>

Hydrogels can be categorized into various types (Fig. 2).<sup>95</sup> Based on the origin of the synthesized materials, they can be classified as natural, synthetic, or hybrid.<sup>96,97</sup> Depending on their polymeric composition, hydrogels can be organized into homopolymer, copolymer, and semi-interpenetrating networks.<sup>65</sup> Hydrogels can be classified as amorphous, crystalline, or semi-crystalline based on their configuration or structure.<sup>98</sup> Hydrogels can be smart or conventional depending on their responsiveness to stimuli.<sup>99</sup> They are also classified as durable, degradable, or biodegradable.<sup>100</sup> Based on their net ionic charge, hydrogels can be classified as cationic, anionic, neutral or ampholytic.<sup>65,101</sup>



Yu-Shuan Chen

bridge materials science and healthcare to make a positive impact on patients' lives.

Dr Yu-Shuan Chen is a research assistant at Tzu Chi Medical Foundation, with a PhD in Chemical Engineering from National Tsing Hua University in Taiwan. Her expertise is in applying materials effectively to biotechnology, particularly in the field of neuroscience therapy and drug delivery. She work on improving treatments for brain cancer and cerebellar atrophy, using various biomedical materials and delivery methods. Her goal is to



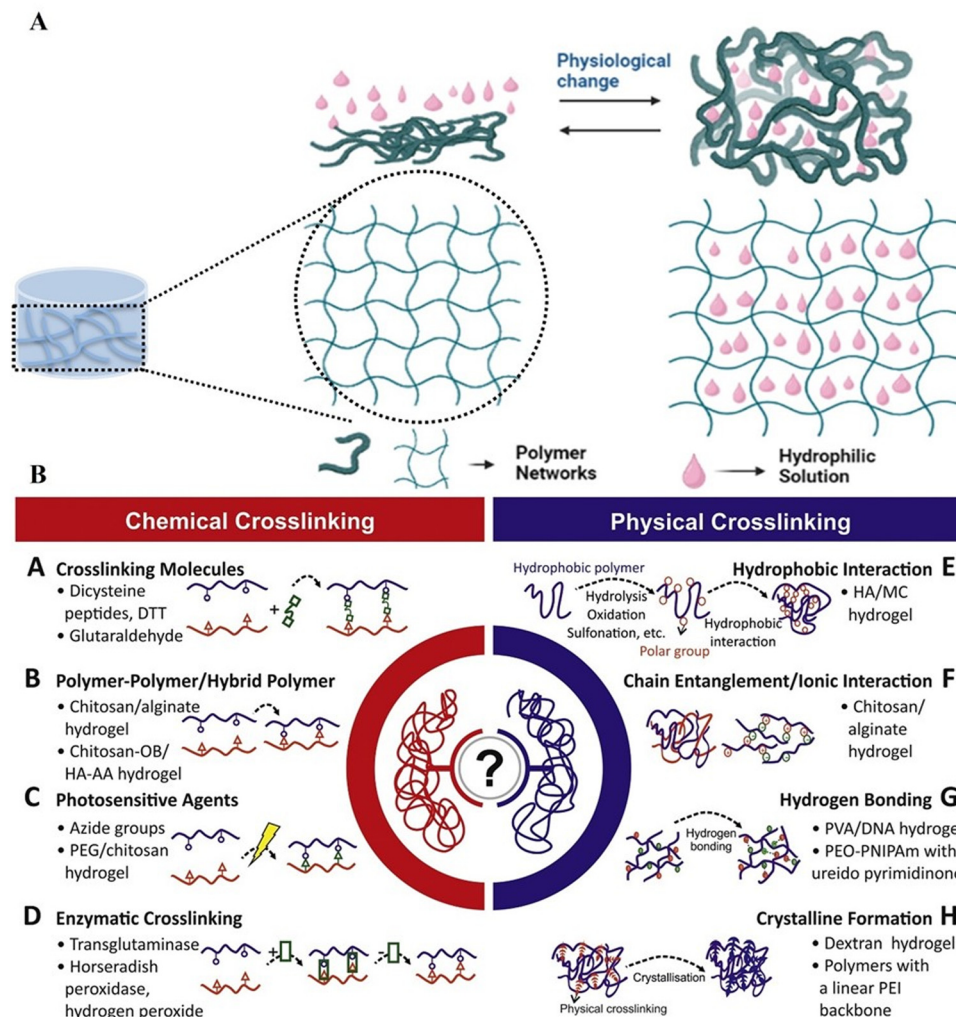


Fig. 1 (A) The transition between swelling and deswelling of nearby stimuli-sensitive hydrogels. (B) Chemical and physical crosslinking types of hydrogels and their chemical sources. Image (B) reprinted from ref. 77 with permission from the publisher (Copyright Elsevier B.V., 2023).

Commonly used naturally derived hydrogels include cellulose, chitosan, alginate, xyloglucan, agarose, and elastin/protein.<sup>92,95,102–104</sup> They are naturally and biochemically compatible with human tissues. However, they exhibit low mechanical strength, challenges in accurate drug formulation and loading, and immunogenic risks.<sup>105,106</sup> Popular synthetic hydrogel polymers, synthesized by blending monomers, include PEG, PEO, polyvinyl alcohol, peptides, and DNA.<sup>107–109</sup> Unlike naturally derived hydrogels, synthetic polymers display high water absorption capacity, well-organized structure, and smart stimuli responsiveness. Furthermore, the properties of synthetic hydrogels, such as mechanical, diffusive, and loading capacities, can be fine-tuned to design drug carriers.<sup>110</sup> Consequently, synthetic hydrogels outperform natural hydrogels in pharmacological applications.<sup>111</sup>

## 2. Bibliometric analysis of hydrogels as drug carriers for cancer treatment

We examined a bibliometric information about “drug carrier hydrogels for cancer treatment” using VOS viewer (version

1.6.18, Liden University Center for Science and Technology). Scopus sources were gathered through keyword searches. The software could provide mapping tools for the analyzed data, focusing on application of hydrogels.<sup>112,113</sup> Our analysis incorporated bibliometric coupling (countries (Fig. 3A), sources (Fig. 3B), documents (Fig. 3C), and authors (3D)), co-occurrence (index key words (Fig. 3D)), co-authorship (countries (Fig. 3E) and authors (Fig. 3F)), citation (countries (Fig. 3G), sources (Fig. 3H), and authors (Fig. 3I)), and co-citation (cited sources (Fig. 3J) and cited authors (Fig. 3K)). Furthermore, we looked at each measurement's bibliometric ranking to its total link strength (TLS).

### 2.1. Bibliometric coupling

Bibliometric coupling can use to ascertain whether the analyzed articles cite one or more documents in common or not. Fig. 3A displays the bibliometric-coupling map of top 17 countries in 3 clusters, selected from 50 countries, based on meeting threshold of minimum 5 documents of a country and 25 maximum countries per document. Accordingly, the five top bibliometric coupled countries are the USA (62 documents,



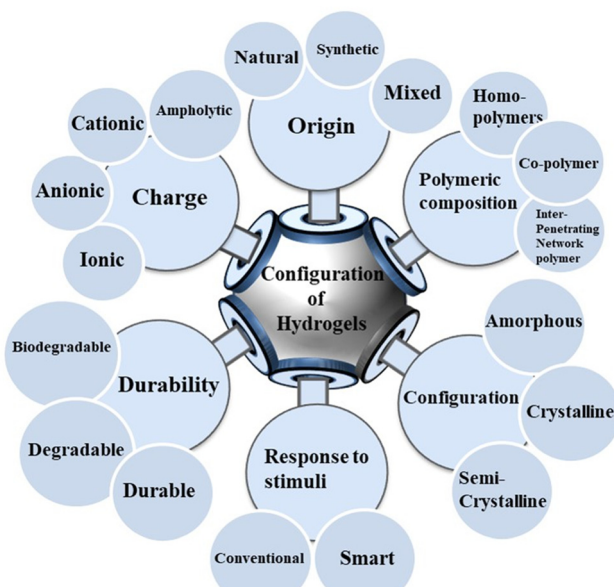


Fig. 2 Schematic view of general classification of hydrogels.

5050 citations, and 5323 TLS), China (87 documents, 2628 citations, and 4062 TLS), Italy (10 documents, 175 citations, and 3263 TLS), Iran (15 documents, 188 citations, and 3094 TLS), and Belgium (5 documents, 193 citations, and 3024 TLS), respectively. Fig. 3B shows a bibliometric-coupling map of 10 sources selected from 146 based on meeting a minimum threshold of 5 documents and 0 citations. The 5 top bibliometrically coupled sources are the Journal of controlled release (13 documents, 756 citations, and 117 TLS), the International Journal of Pharmaceutics (12 documents, 261 citations, and 116 TLS), Biomaterials Science (10 documents, 129 citations, and 102 TLS), Biomaterials (10 documents, 775 citations, and 85 TLS), and Pharmaceutics (7 documents, 266 citations and 58 TLS), respectively. We also analyzed the bibliometric coupling of 282 documents (Fig. 3C) met the criteria of a minimum 0 citations and five maximum authors per document. The 5 top bibliometric coupled documents are Riley R. S. (2019) (1108 citations and 101 TLS), Song R. (2018) (470 citations and 34 TLS), Bidarra S. J. (2014) (378 citations and 533 TLS), Conde J. (2016) (347 citations and 12 TLS), and Venditto V. J. (2010) (323 citations and 24 TLS), respectively. Finally, we analyzed the bibliometric coupling of authors, and Fig. 3D presents the bibliometric coupling of top 14 authors qualified a threshold of five minimum documents of an author and 25 maximum number of authors per document. Accordingly, the top 5 bibliometric coupled authors are Wang Y. (6 documents, 81 citations, and 938 TLS), Xu X. (5 documents, 165, and 912 TLS), Zhang H. (5 documents, 133 citations, and 885 TLS), Li W. (5 documents, 223 citations, and 697 TLS), and Chen X. (6 documents, 260 citations, and 390 TLS), respectively.<sup>114</sup>

## 2.2. Co-occurrence analysis

We conducted an index keyword co-occurrence analysis to identify areas of interest within the hydrogels field.<sup>114</sup>

First, we analyzed the relatedness of items based on the number of items cited by each other. Fig. 3E presents an index keyword co-occurrence of 422 keywords selected from 4323, based on meeting a minimum threshold of five keyword occurrences. The five most frequently occurring index keywords are hydrogel (195 times, TLS = 6132), drug delivery systems (174 times, TLS = 5344), Chemistry (85 times, TLS = 3069), controlled study (80 times, TLS = 2897), and drug delivery systems (89 times, TLS = 2897). The four colors of the clusters observed in the analysis represent various areas identified after filtering using the VOS viewer software. The investigation shows that the most popular and recent application of hydrogels is drug delivery, dominated by cancer therapy.

## 2.3. Co-authorship analysis

Co-authorship analysis based on citations helps to identify highly cited authors, particularly those within the same research area.<sup>115</sup> We analyzed co-authorship among countries and authors, focusing on hydrogels anti-cancer drug delivery applications. Fig. 3F presents co-authorship of 17 countries selected from 50 based on meeting a threshold of five minimum documents of a country, 25 maximum countries per document, and zero minimum citations. The top five co-authored countries are China (87 documents, 2628 citations, and 25 TLS), USA (62 documents, 5065 citations, and 24 TLS), Iran (10 documents, 188 citations, and 14 TLS), Italy (10 documents, 175 citations, and 14 TLS), and Canada (11 documents, 183 citations, and 11 TLS). To perform co-authorship analysis based on authors, we limited our analysis to a maximum of 25 authors per document, five minimum documents of an author, and zero minimum citations of an author. Out of the 1403 selected authors, 14 met these criteria. We analyzed each author's total co-authorship link strength with other authors and identified those with the strongest links. The top 5 highly co-authorship authors are Chen X. (6 documents, 260 citations, and 7 TLS), Li W. (5 documents, 223 citations, and 7 TLS), Zhang H. (5 documents, 133 citations, and 7 TLS), Liu X. (5 documents, 252 citations, and 6 TLS) and Li Y. (12 documents, 290 citations, and 5 TLS), respectively (Fig. 3G).

## 2.4. Citation analysis

Vos viewer citation analysis uses to identify how often the published work is cited. Therefore, we analyzed citations of selected articles based on countries, sources, and authors. We performed a citation map of 17 countries chosen from 50 based on fulfilling the minimum threshold of 5 documents of a country, 0 citations, and 25 maximum number of countries per document. The map contains 16 items classified into 5 clusters (Fig. 3H). The top 5 cited countries are China (87 documents, 2628 citations, and 35 TLS), the USA (62 documents, 5065 citations, and 35 TLS), the Netherlands (8 documents, 205 citations, and 10 TLS), United Kingdom (16 documents, 839 citations, and 10 TLS), and India (36 documents, 946 citations, and 8 TLS) respectively. We also analyzed citations



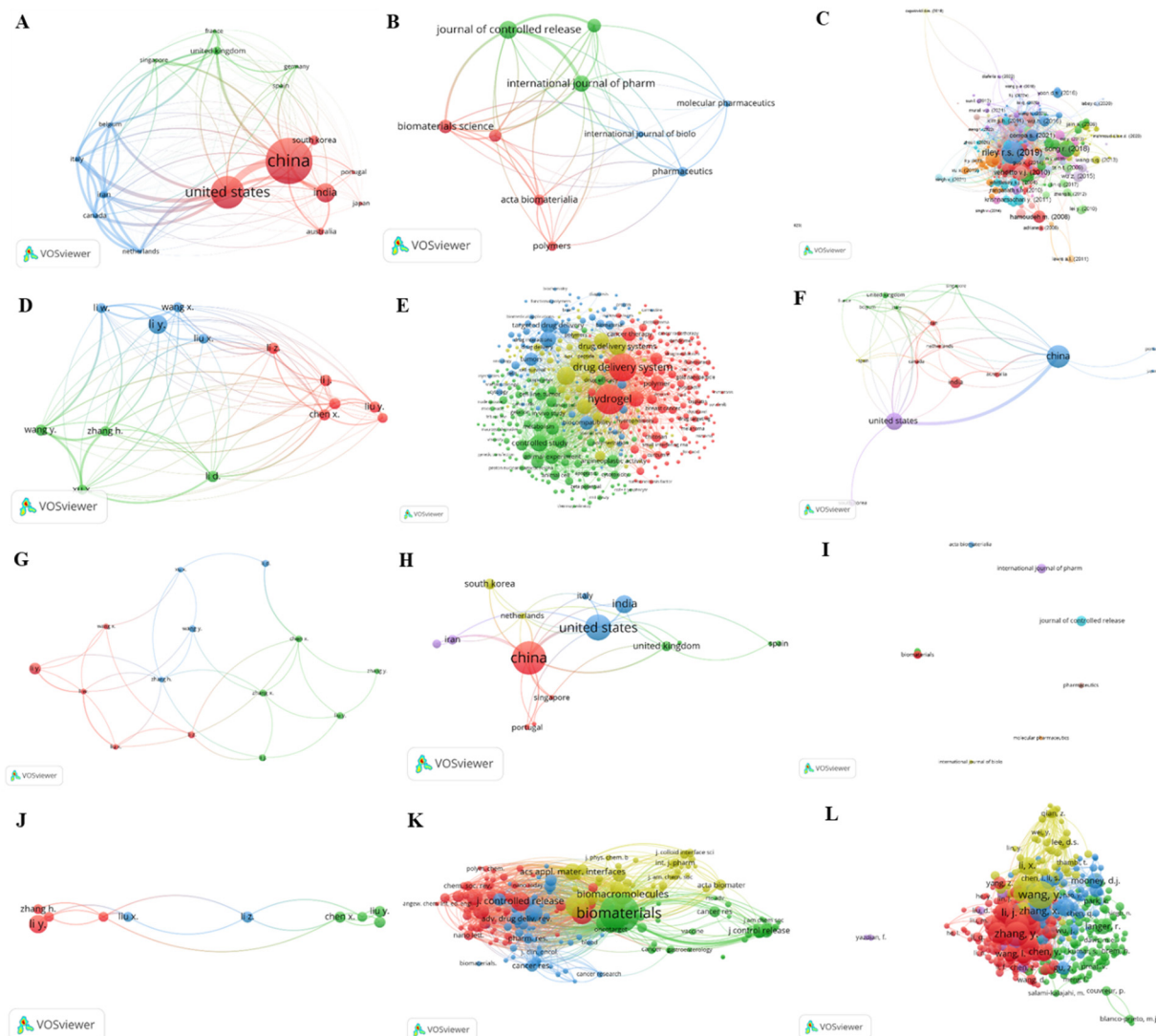


Fig. 3 VOS viewer bibliometric analysis of hydrogels as cancer drug carrier tools.

based on sources. Fig. 3I displays a citation map of the top 10 sources, classified into 4 clusters, selected out of 146 sources based on a minimum qualification of 5 documents of a source and 0 citations. The top five cited sources are *ASC applied materials and interfaces* (9 documents, 652 citations, and 3 TLS), *Biomaterials* (10 documents, 775 citations, and 3 TLS), *Biomaterials science* (10 documents, 129 citations, and 3 TLS), *Polymers* (7 documents, 266 citations, and 1 TLS), and *Acta Biomaterialia* (8 documents, 47 citations, and 0 TLS), respectively. We further analyzed citations based on authors to identify the highly cited author in hydrogels for cancer drug delivery. Thus, Fig. 3J presents citation mapping of the top 10 authors in 3 clusters, selected from 1403 based on a minimum qualifying threshold of 5 documents of an author and 25 maximum authors per document. The five most cited authors are Wang X. (5 documents, 120 citations, and 7 TLS), Chen X. (6 documents, 260 citations, and 5 TLS), Li W. (5 documents, 223 citations, and 4 TLS), Li Z. (6 documents, 174 citations, and 4

TLS), and Liu X. (5 documents, 252 citations, and 4 TLS), respectively.

## 2.5. Co-citation analysis

We conducted a cocitation analysis to identify articles frequently cited by other articles. Accordingly, we analyzed the cocitation of cited sources and authors to determine the top most cited journals and authors in the area of hydrogels for cancer drug delivery. Fig. 3K presents the cocitation mapping of 196 cited sources in four clusters, selected from 5811 sources based on a minimum threshold of 20 citation sources. The top five co-cited sources are *Biomaterials* (952 citations and 72 705 TLS), *Journal of controlled release* (263 citations and 31 796 TLS), *Biomacromolecules* (308 citations and 24 998 TLS), *ACS Nano* (306 citations and 24 170 TLS), and *Journal of American Chemical Society* (196 citations and 19 712 TLS). Furthermore, we analyzed the cocitation of cited authors to determine the most co-cited authors. Fig. 3L displays a cocitation analysis of the top 401



authors in five clusters, qualified from 54 423 authors based on a minimum threshold of 20 citations of an author. The top 5 co-cited authors are Wang Y. (367 citations and 59 208 TLS), Zhang Y. (292 citations and 46 312 TLS), Li J. (255 citations and 44 888 TLS), Wang J. (279 citations and 43 987 TLS), and Li Y. (243 citations and 36 779 TLS).

### 3. Drug carrier hydrogels and their stimuli responsiveness

Recently, stimuli-responsive hydrogels have garnered considerable interest due to their vast potential in both *in vitro* and *in vivo* drug delivery applications.<sup>116</sup> These hydrogels can carry and release drugs once inside cells. To accomplish this, smart hydrogels must withstand the intracellular microenvironment and safeguard the drug until the desired release kinetics are achieved.<sup>117,118</sup> The protection of the loaded drug from denaturation, aggregation, and other micro environmental reactions is managed by these cross-linked structures, which form a solid-like gel that prevents interactions between the drug and surrounding materials.<sup>119</sup> For instance, the cross-linked structure of hydrogels can hinder the infiltration of various proteins, including drug-degrading enzymes, thereby preventing premature drug degradation.<sup>118</sup> Moreover, owing to their biodegradability and non-toxicity when breaking down their 3D cross-linked networks, smart hydrogels have attracted tremendous interest for drug delivery.<sup>70</sup>

Smart hydrogels, synthesized from synthetic and natural polymers, can alter their properties upon exposure to external or internal stimuli, such as temperature, pH, light, ion change, redox potential, magnetic fields, electric fields, and chemical molecules (e.g., glucose, ligands, and ROS) (Fig. 4).<sup>120–122</sup> Stimuli-responsive

properties of hydrogels originate from the presence of interactive functional groups such as carboxyl, amide, sulfonic groups, and structures with functional groups such as acryl amide, (3-acrylamidopropyl)trimethyl-ammonium chloride (APTMACl), and 2-acrylamido-2-methyl-1-propanesulfonic acid (AMPS), within the primary polymeric chains (Fig. 5). Thus, the synthesis of smart hydrogels considers the stimuli-responsive nature of the active functional groups attached to the main chain.<sup>70,123</sup> Other functional groups, including amidoxime, phosphoramidate, phosphine, and phosphate, also contribute.<sup>124,125</sup> When these functional groups respond to stimuli, hydrogels shrink or swell, bend or degrade, and form a gel, solution, or precipitate, which can be employed to design stimuli-responsive hydrogels as required. This response can be readily confirmed by observing changes in the physical properties of the networks.<sup>126,127</sup> Additionally, the stimuli-responsive behavior of smart hydrogels is also attributed to other types of bonding or interactions. Among these, well-known physical interactions include hydrophobic, ionic, H bonding and van der Waals forces.<sup>128,129</sup> Apart from the active functional groups, physical interactions are responsible for the interconversion between solution and gel states. Although the presence of functional groups primarily imparts the stimuli-responsive nature of the hydrogel, the extent of the response depends on the type of these groups and the repeating unit of the base polymer. In the case of copolymers, the composition of these units and the number of ionizable functional groups in the main chain impact the response.<sup>130,131</sup>

### 4. Thermal sensitive hydrogels

#### 4.1. Behavior of thermal sensitive hydrogels

Thermally-sensitive hydrogels are the most researched stimuli-responsive hydrogels for drug delivery applications.<sup>133</sup> They

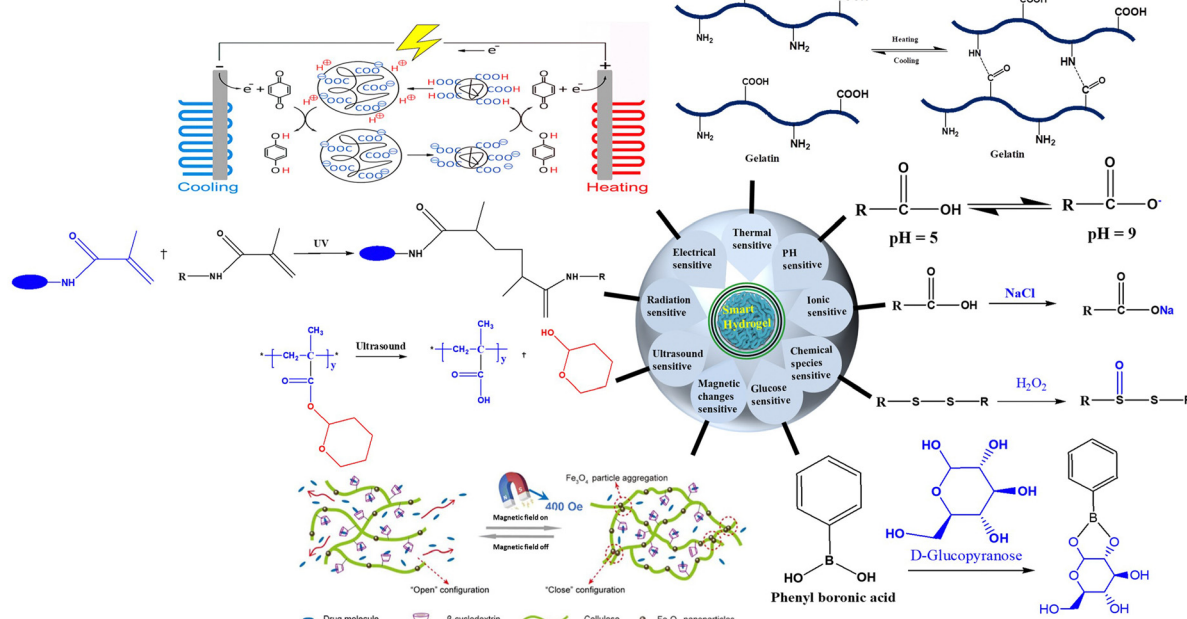


Fig. 4 Classification of smart hydrogels based on response to stimuli.<sup>132</sup>



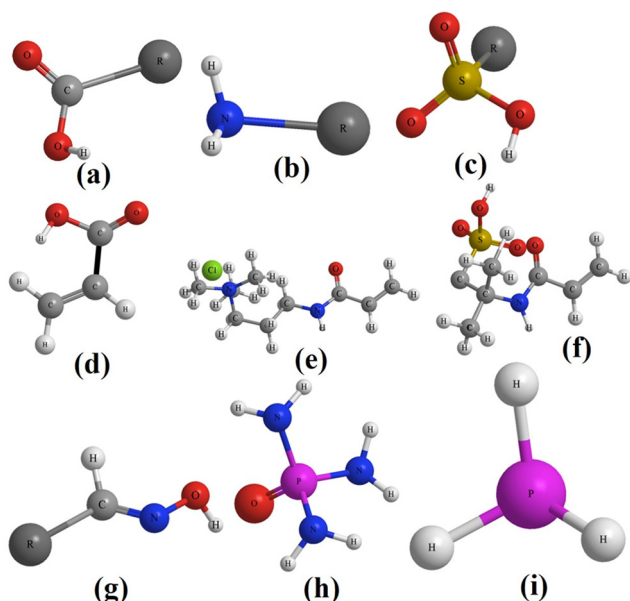


Fig. 5 Ball and stick structure of functional groups on the surface of drug carrier hydrogels related to stimulus-response; (a) carboxyl, (b) amine, and (c) sulfonic groups. Monomers with a similar functional group on their surface; (d) acrylamide, (e) APTMAcI, and (f) AMPS. Lewis structure of other functional groups available on the surface of hydrogels; (g) amidoxime, (h) phosphoramido, and (i) phosphine.

have recently received increased interest due to their gel-forming ability under physiological conditions ( $\text{pH} = 7.4$  and  $T = 37^\circ\text{C}$ ).<sup>134,135</sup> Moreover, they possess specific CSTs that exhibit phase transition properties in hydrophilic environments.<sup>136</sup> These hydrogels' characteristics are determined by the hydrophobic to hydrophilic ratio within the polymer matrices that constitute them.<sup>137,138</sup> Various hydrophobic groups, such as methyl, ethyl, and propyl groups, offer superior thermal properties to hydrogels compared to other groups.<sup>139</sup> Temperature fluctuations cause the hydrogels to swell or contract, inducing changes in the polymer structure and phase transition. This leads to the adjustment of the release of encapsulated drugs.<sup>140–142</sup> The drugs are loaded onto thermosensitive hydrogels by mixing them with hydrogel solutions at low temperatures, which prevents the loss of the natural structure of the drug materials.<sup>143</sup> However, the strength and stability characteristics of the hydrogels and encapsulated drugs change with environmental temperature variations.<sup>144</sup> Generally, these hydrogels have thermoresponsive phase transition features and are designed using diverse strategies to regulate and control the temperature *in vivo*.<sup>145,146</sup>

Thermally sensitive hydrogels can be categorized into two temperature-dependent systems that exhibit structural changes. These include the upper critical solution temperature (UCST) and lower critical solution temperature (LCST).<sup>147–149</sup> Hydrogels derived from polymer solutions with LCST characteristics form a single-phase solution below the LCST and transition to a gel with a turbid, two-phase solution at or above the LCST.<sup>150,151</sup> As amphiphilic macromolecules, LCST hydrogels can restructure themselves into micelles when their

concentration surpasses the CMC. Below the LCST, micelles are relatively large due to the hydration of hydrophilic components, with hydrophobic blocks forming the micelle core and hydrophilic elements creating the shell (Fig. 6C). As the temperature rises, hydrophilic chains dehydrate, micelle size decreases, hydrophobic and van der Waals interactions increase, hydrophilic connections cluster, and a phase transition occurs at the LCST, resulting in two solution phases.<sup>152</sup> This demonstrates that hydrophobic and hydrophilic interactions are fundamental to the sol-gel process. In contrast, hydrogels made of UCST polymers form a single-phase solution above their UCST while contracting and generating a turbid solution at or below their UCST (Fig. 6B).<sup>153,154</sup> As the temperature increases, UCST hydrogels become more soluble in water, forming large micelles with hydrophobic cores and *vice versa* (Fig. 6C). In both cases, shrinkage is caused by hydrogel dehydration in response to temperature changes. By contrast, swelling is caused by hydrogel hydration in response to thermal variations.<sup>155,156</sup>

#### 4.2. Steps for the synthesis of thermal sensitive hydrogels

Synthesis of thermal sensitive hydrogels involves crosslinking of monomers that are responsive to temperature. The process has requirements, specific steps and reactions.<sup>127</sup>

**4.2.1. Requirements for synthesis of thermal sensitive hydrogels.** (1) Monomers; – the initial step in the synthesis involves selecting monomers with thermally sensitive properties. The most commonly utilized monomers include *N*-isopropyl acrylamide (NIPAAm), polyethylene glycol (PEG), poly(*N*-vinyl caprolactam) (NVCL), poly(*N*-vinylpyrrolidone) (PVP), poly(ethylene oxide-*co*-propylene oxide) (PEO-PPO-PEO), polyurethanes, poly acrylic acid (PAA), and poly(2-oxazoline).<sup>157,158</sup>

(2) Crosslinking agents; – play a crucial role in forming the 3D network of the hydrogel. Although the choice of the crosslinking agent depends on the specific requirements of the hydrogel, including its intended applications and the desired response to temperature changes.<sup>159</sup> Commonly used crosslinking agents include *N,N'*-methylene bis(acrylamide) (MBA), *N,N'*-diethyl acrylamide (DEAA), poly(ethylene glycol)diacrylate (PEGDA), poly(ethylene glycol)dimethacrylate (PEGDMA), 1,6-hexanediol diacrylate (HDDA), ethylene glycol dimethacrylate (EGDMA), and divinyl sulfone (DVS).<sup>160</sup>

(3) Initiators; – chemical synthesis employs a variety of initiators to kick-start or catalyze the process. These initiators encompass chemical agents like azobisisobutyronitrile and potassium persulfate, heat as a thermal initiator, redox initiators such as ammonium persulfate (APS) paired with *N,N,N',N'*-tetramethylethylenediamine (TEMED), photoinitiators like benzoin methyl ether, enzymatic initiators exemplified by horse radish peroxidase, and unconventional methods such as microwave or ultrasonic initiators, as well as electrochemical initiators that furnish electrons to instigate the chemical reaction.<sup>161</sup>

(4) Solvents; – the choice of solvents relies on the specific polymers or monomers in use and their compatibility. Additionally, co-solvents may be employed depending on the nature of the required monomers for synthesis. With this principle in mind, commonly utilized solvents for synthesizing thermally

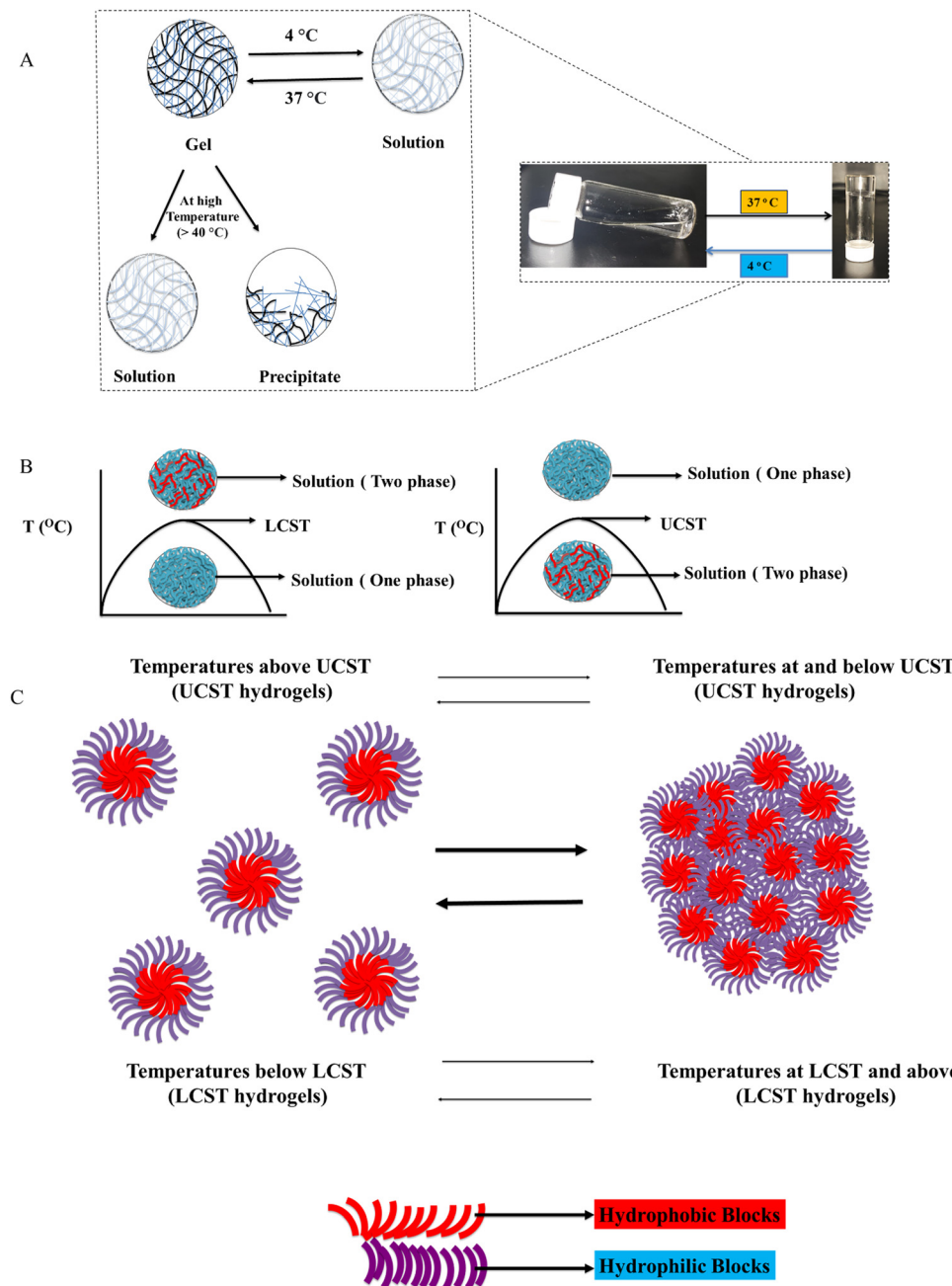


Fig. 6 (A) Diagrammatic representation of thermally sensitive hydrogels and their temperature-induced physical changes and (B) solution nature of hydrogels constructed from polymers with LCST (left) and UCST (right). (C) Diagrammatic illustration of thermal responsiveness in LCST and UCST hydrogels.

sensitive hydrogels include water, dimethyl sulfoxide (DMSO), *N,N*-dimethylformamide (DMF), ethanol, acetone, acetonitrile, tetrahydrofuran (THF), and hexane.<sup>162</sup>

(5) Temperature controlling equipment: – used to maintain specific reaction temperature.<sup>163</sup>

**4.2.2. Synthesis steps and reactions.** (1) Monomer dissolution; – to initiate the desired polymerization process, ensure complete dissolution of monomers in the selected solvent or co-solvent.<sup>164</sup>

(2) Crosslinking agent addition; – add the chosen crosslinking agent to the dissolved monomer solution to facilitate crosslinking and create a three-dimensional network.<sup>163</sup>

(3) Addition of initiator; – used to initiate the polymerization reaction in response to temperature changes.<sup>165</sup>

(4) Polymerization reaction; – upon initiation, the hydrogel synthesis can proceed through various methods tailored to specific needs: free radical polymerization (either chain growth or step-growth polymerization), inverse emulsion polymerization, or controlled/living radical polymerization. The two most prevalent techniques for hydrogel synthesis are chain growth and step growth polymerizations.<sup>166</sup>

In chain-growth polymerization, the process kicks off with an initiator either a chemical compound or a physical stimulus



such as light, radiation, or heat. This initiates the creation of reactive species (radicals) that kick start the polymerization. Subsequently, monomers join in, propagating with the reactive species to forge the expanding polymer chain until all reactive species are consumed, terminating the reaction.<sup>167</sup>

Step growth polymerization involves activating monomers to generate reactive species, followed by their covalent interaction to construct the necessary polymer until the reaction terminates. These versatile methods provide a nuanced approach to crafting hydrogels, offering flexibility and precision in their synthesis.<sup>168</sup>

(5) Purification of the synthesized hydrogel: – purifying synthesized hydrogels involves eliminating impurities, unreacted monomers, and other substances that may reside in the hydrogel matrix.<sup>169</sup> The choice of the purification method depends on the specific hydrogel type and the polymerization technique utilized. General purification methods for polymerized hydrogels include employing solvent extraction, dialysis, centrifugation, filtration, precipitation, chemical treatments, or combinations thereof.<sup>170</sup>

#### 4.3. Selected synthetic thermal sensitive hydrogels

##### 4.3.1. Poly(*N*-isopropyl acryl amide) (PNIPAM) hydrogels.

Most LCST hydrogels utilized in drug delivery applications are primarily produced through polymerization or copolymerization to ensure an effective drug delivery.<sup>33,171</sup> PNIPAM and its copolymers are the most extensively studied polymers with LCST properties.<sup>172,173</sup> The benefits of PNIPAM, such as low bio-toxicity, temperature sensitivity, and easily modifiable architecture, make it an ideal candidate for drug delivery applications.<sup>174</sup> PNIPAM comprises hydrophobic isopropyl side chains ( $-\text{CH}(\text{CH}_3)_2$ ) and hydrophilic amide groups ( $-\text{CONH}$ ) (Fig. 5).<sup>175</sup> The hydrophilic H bonding interaction between the *N*-alkyl-substituted group and water molecules results in a moderate swelling response in PNIPAM hydrogels (homogeneous solution) (Fig. 7A and C).<sup>176,177</sup> This process initiates with the forming of water cages that hydrate the hydrophobic segments of PNIPAM. These cages counterbalance the insolubility of the hydrophobic backbone in water, resulting in polymer hydration (swelling). Throughout this process, PNIPAM forms a reversible temperature-sensitive layer on the gel surface.<sup>178</sup> The LCST of PNIPAM is  $32\text{ }^\circ\text{C}$ , which is close to physiological temperature, and it maintains a single-phase solution up to this point.<sup>158,179</sup> When the temperature reaches  $32\text{ }^\circ\text{C}$ , the hydrophilic layers between the polymer and water molecules rupture, causing deswelling and forming hydrophobic precipitates. PNIPAM hydrogels are employed to release drugs at their LCST. However, copolymerization helps create copolymer hydrogels and modifies LCST values and gel formation (Fig. 7B).<sup>180,181</sup> Hydrophilic comonomers, such as acrylamide, raise the LCST, while hydrophobic comonomers tend to decrease it. For instance, a copolymer of PNIPAM and acrylamide exhibits an LCST at physiological temperature ( $37\text{ }^\circ\text{C}$ ).<sup>182,183</sup> Furthermore, hydrogels generated by copolymerizing PNIPAM with ionic moieties exhibit both pH and temperature-sensitive properties, making them more precise carriers for localized cancer treatment.<sup>184,185</sup>

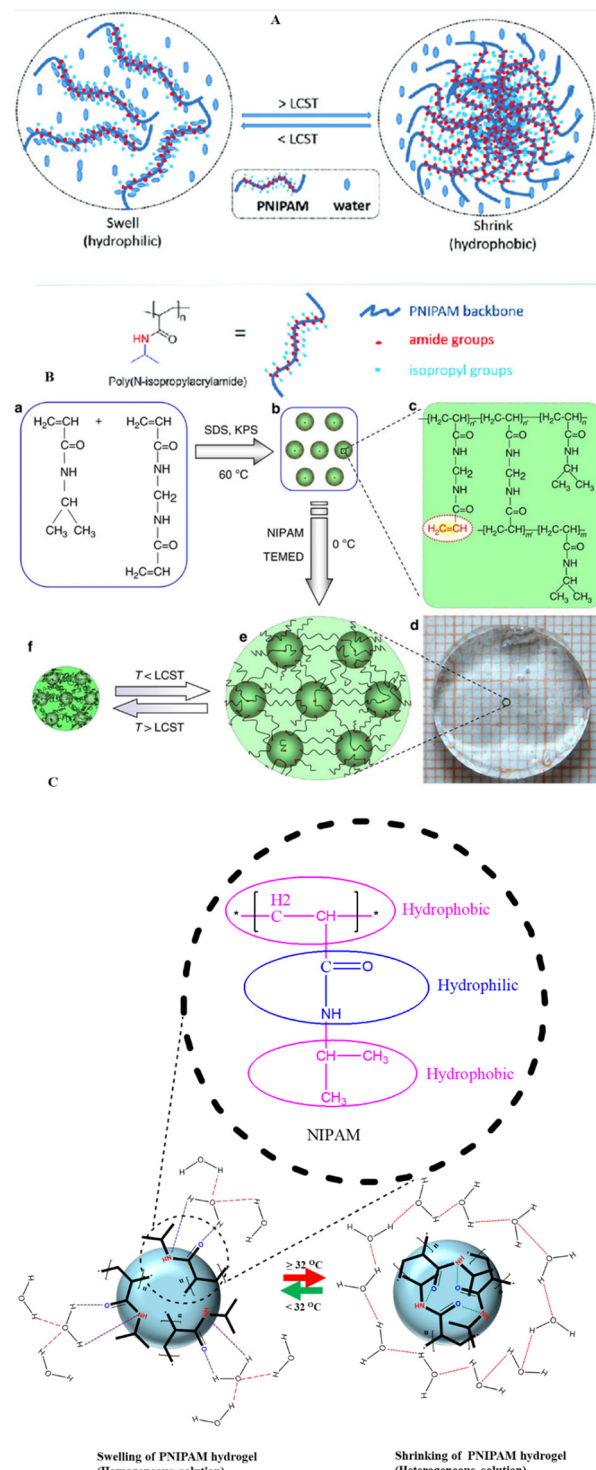
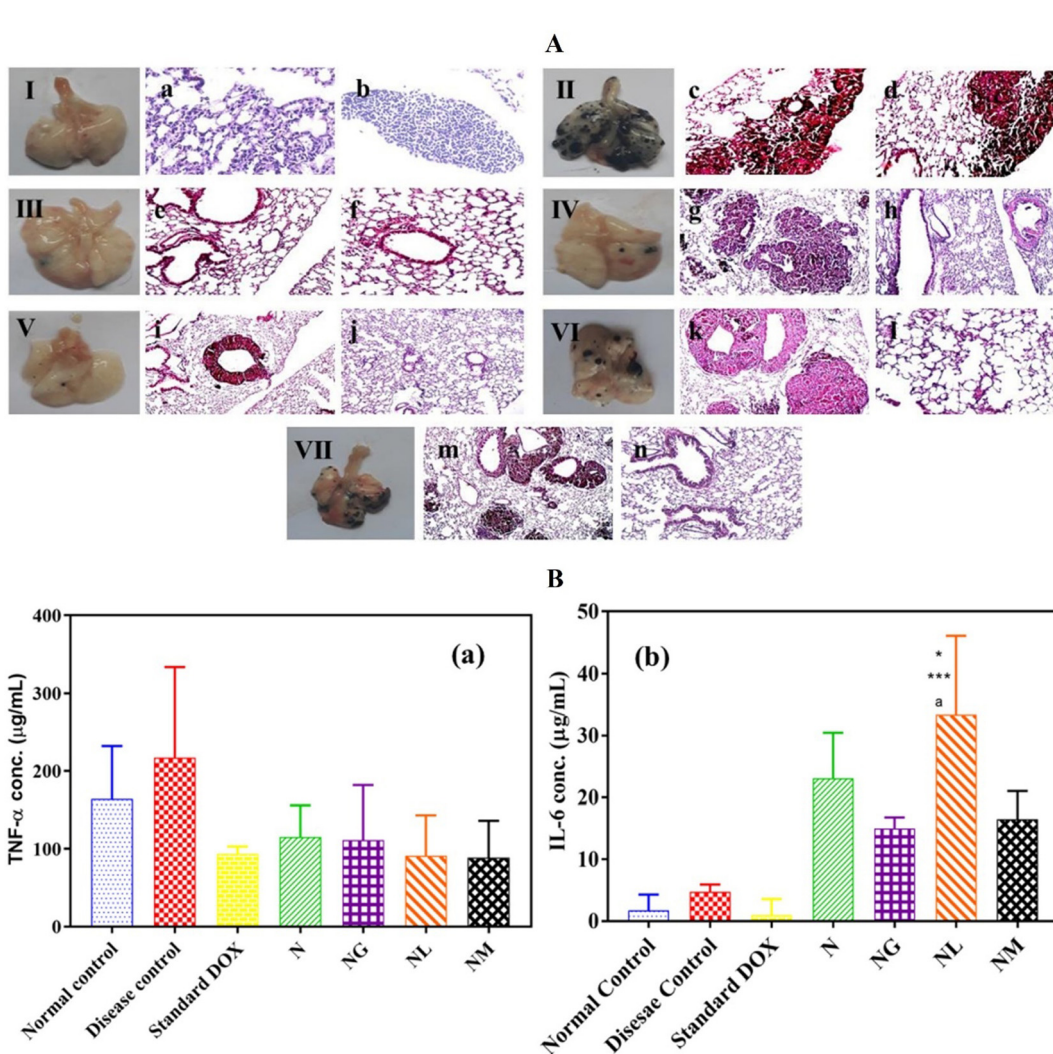


Fig. 7 (A) Schematic view of temperature dependent sol gel transition of NIPAM based hydrogel. (B) Chemical structures of PNIPAM and *N,N* methylene bis acrylamide (MBA) (a), copolymer of NIPAM and MBA synthesized by precipitation polymerization (b), Structure of the synthesized activated NIPAM based nano gel (c), optical image of the hydrogel constructed from NIPAM and activated nanogel at low temperature (d), schematic of the copolymer hydrogel at temperature  $<$  LCST (e) and  $>$  LCST (f). (C) Diagrammatic illustration of swelling (hydration) and shrinkage (precipitate formation) of PNIPAM hydrogel. (A) is adapted from ref. 186 and (B) from ref. 187 (with permission of the publisher copyright Royal Society of Chemistry 2023).



**4.3.1.1. Thermal-sensitive PNIPAM hydrogels used in local drug delivery.** To address the cytotoxicity and high-dosage concerns related to cancer treatment medications, the methodical design of thermally sensitive hydrogels using natural, synthetic, or mixed monomers is crucial.<sup>188</sup> The site-specific drug release provided by these hydrogels can exploit tumor microenvironments that differ from normal cells, such as elevated temperatures and acidic pH.<sup>189</sup> PNIPAM is a widely utilized thermally sensitive hydrogel for delivering chemotherapeutic, immunotherapeutic, photodynamic, and other medications to treat various cancer types.<sup>33,190,191</sup> Over the past decade, local drug delivery with PNIPAM hydrogels has led to improved drug loading capacity, reduced rapid drug release, and fewer adverse therapeutic effects.<sup>192,193</sup> Particularly, the

intratumoral injection of drugs carried by PNIPAM based hydrogels results in decreased drug diffusion to nonspecific organs and related side effects.<sup>194</sup> DOX, a chemotherapeutic drug, functions by inhibiting the activity of the topoisomerase II enzyme in cancer cells. This enzyme plays a crucial role in the replication process by preventing the supercoiling of parental DNA.<sup>195,196</sup> However, the action mechanism of DOX leads to the generation of quinone-type free radicals, resulting in significant cytotoxic side effects.<sup>197,198</sup> Employing smart thermally sensitive PNIPAM hydrogel carriers for local drug delivery mitigates the adverse effects of DOX.<sup>191,199</sup> A recent study in a mouse model employed GQDs, LGQDs, and MGQDs functionalized PNIPAM hydrogels to deliver DOX to BF16F melanoma tumors, which can metastasize to lung cells.<sup>200</sup> This



**Fig. 8** (A) Resected lung tissues from seven different study groups of mice: (I) standard control, (II) disease control, (III) treated with standard DOX, (IV) treated with NDOX, (V) treated with DOX- and NG-DOX, (VI) treated with DOX and leucine-modified GQDs-loaded nano hydrogel (NGL-DOX), and (VII) treated with DOX and methionine-modified GQDs-loaded nano hydrogel (NGM-DOX). Histopathology of resected lung tissues from the seven study groups of mice: (a) and (b) normal controls in the complete absence of tumor cells, (c) and (d) disease controls display melanin-producing colonies, (e) and (f) DOX-treated group showing no tumor formation, (g) NDOX-treated groups displaying metastasized melanoma, (h) and normal lung parenchyma. (i) NG-DOX-treated groups showing melanoma-affected lung bronchus and (j) abnormal lung parenchyma (j). NGL-DOX-treated groups revealing the appearance of melanoma (k) and regular lung parenchyma (l). (B) Serum TNF- $\alpha$  (B(a)) and IL-6 (B(b)) levels of the seven groups of mice. Images reprinted from ref. 200 with permission from the publisher (order license ID: 1165618-2, 27 March 2023).



Table 1 Selected poly(*N*-isopropyl acrylamide) (PNIPAM)-based thermally sensitive hydrogels and their potential as drug carriers for various cancer types

Name of PNIPAM family hydrogel	Structure/s of the hydrogel	Monomers used	LCST of the drug used for hydrogel delivery	Type of cancer	Earned benefits of copolymerization drug alone)	Advantage of using the hydrogel (in comparison with the drug alone)	Ref.
Poly(carboxymethyl chitosan-grafted-isopropyl acryl amide) (CMCS- <i>g</i> -NPAAm)		Carboxymethyl chitosan and PNIPAM	37 °C	5-Fluoro uracil HeLa (cervical cancer) and MCF <sub>7</sub> (breast cancer)	✓ Increased mechanical strength and intra-cellular stability	✓ Drug release at acidic PH	202
Carboxymethyl fenugreek galactomannan- <i>g</i> -poly( <i>N</i> -isopropyl acrylamide- <i>co</i> - <i>N,N</i> '-methylene-bis-acrylamide)		Fenugreek galactomannan and poly( <i>N</i> -isopropyl acrylamide- <i>co</i> - <i>N,N</i> '-methylene-bis-acrylamide)	37 °C	Erlotinib A549 cells (lung cancer)	✓ Enhanced mechanical strength and biodegradability	✓ Highest drug loading efficiency	203
Poly( <i>N</i> -isopropyl acrylate- <i>co</i> -acrylic acid) (P(NIPA- <i>co</i> -AA))		PNIPAM and acrylic acid	37 °C	5-Aminolevulinic acid HeLa (cervical cancer)	✓ Increased mechanical strength	✓ Less cytotoxicity	204
Chitosan- <i>g</i> -poly( <i>N</i> -isopropyl acrylamide) (CS- <i>g</i> -PNIPAM)		PNIPAM and chitosan	39 °C	Capecitabine HCT116 and HT-29 (colon cancer)	✓ Improved mechanical resistance in acidic PH	✓ Significantly increased drug release	189
						✓ Minimal side effects	



Table 1 (continued)

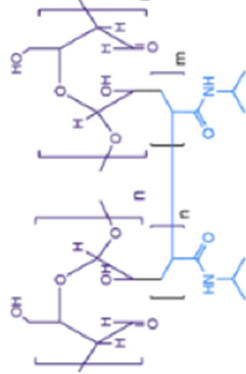
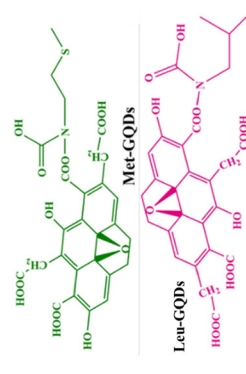
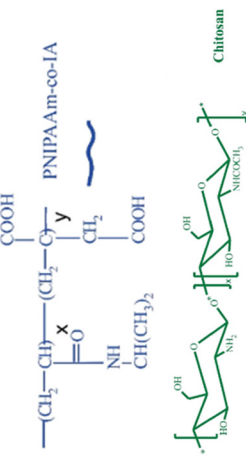
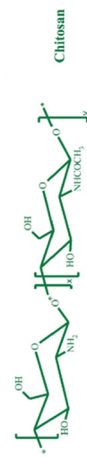
Name of PNIPAM family hydrogel	Structure/s of the hydrogel	Monomers used	LCST of An anticancer drug used for hydrogel delivery	Type of cancer	Earned benefits of copolymerization drug alone	Advantage of using the hydrogel (in comparison with the copolymerization drug alone) Ref.
NIPAM-cellulose		NIPAM and cellulose	37 °C	Doxorubicin and niclosamide	✓ Enhanced mechanical stability and LCST	✓ Incorporation of both hydrophobic and hydrophilic drugs
Poly( <i>N,N</i> -diethyl acrylamide)/functionalized graphene quantum dots		PNIPAM and graphene quantum dots	36 °C	Doxorubicin	✓ Enhanced LCST and anti-cancer activity of the gel	✓ Improved LCST and anti-cancer activity of the gel
Chitosan/(poly( <i>N</i> -isopropyl acrylamide-co-itaconic acid))		Poly( <i>N</i> -isopropyl acrylamide-co-itaconic acid and chitosan)	39 °C	Doxorubicin	✓ Gaining dual properties (PH and thermal)	✓ Improved sustain capacity
		Chitosan				✓ Enhanced biocompatibility and biodegradability



Table 1 (continued)

Name of PNIPAM family hydrogel	Structure/s of the hydrogel	Monomers used	LCST of the hydrogel delivery	An anticancer drug used for hydrogel delivery	Type of cancer	Benefit of copolymerization drug alone	Advantage of using the hydrogel (in comparison with the copolymerization drug alone) Ref.
Poly( <i>N</i> -isopropyl acrylamide)-co-poly( <i>N,N</i> -dimethylamino)ethyl methacrylate)		NIPAM and <i>N,N</i> -dimethylaminoethyl methacrylate)	39 °C	Cisplatin	HepG2 (hepatocellular carcinoma)	✓ Enhanced cytotoxicity of HepG2 cells	✓ Improved drug delivery 207
Poly( <i>N</i> -isopropyl acrylamide)- <i>b</i> -poly(L-histidine)		NIPAM and histidine	37 °C	Doxorubicin	HepG2/hepatocellular carcinoma)	✓ Exhibit LCST value at physiological temperature	✓ Higher drug loading and release
Poly( <i>N</i> -isopropyl acrylamide)- <i>g</i> -carboxymethyl chitosan		CMCS	32 °C	Cisplatin	A549(lung cancer)	✓ Gaining tunability and dual responsive nature (pH and thermal) for controlled drug release	✓ Excellent loading efficiency

histopathological investigation showed that treatment with DOX-loaded LGQDP and MGQDP hydrogels exhibited normal lung parenchyma with fewer visible melanin-forming cells compared to the disease control (Fig. 8A). Additionally, the evaluation of cytokines, serum TNF- $\alpha$ , and IL-6 in LGQDP and MGQDP treated groups confirmed biocompatibility and reduced immunogenicity of the hydrogels (Fig. 8B). Using PNIPAM hydrogels as intertumoral drug carriers may also reduce neutropenia associated with the antineoplastic agent DOX.<sup>201</sup> The advantages and formulations of selected thermo-sensitive PNIPAM hydrogels for treating various cancers have been extensively detailed (Table 1).

**4.3.2. Pluronic based hydrogels.** The food and drug administration (FDA) have approved Pluronic hydrogels, particularly F127, as drug carriers.<sup>210–212</sup> These hydrogels are composed of the polymer PEO–PPO–PEO, also referred to as poloxamer. The PEO–PPO–PEO structure of pluronic is a tri-block ABA-type copolymer, exhibiting an amphiphilic nature owing to the hydrophobic backbone of PPO and the hydrophilic PEO.<sup>210,213</sup> Pluronic possesses disproportionate PEO hydrophilic groups, allowing it to maintain a solution state at lower temperatures. Conversely, gel aggregates form at higher temperatures due to increased interactions with PPO.<sup>214,215</sup> Thermally induced gelation of pluronic occurs because of micelle packing.<sup>216</sup> At lower temperatures, large-sized pluronic micelles with a

hydrophobic PPO core and a hydrophilic PEO shell form due to predominantly hydrophilic interactions between water molecules and PEO chains.<sup>217–219</sup> However, the number of micelles increased the size of micelles decreased, inter-micellar distance reduced, and gel formed due to increasing hydrophobic contact between PPO chains at higher temperatures (Fig. 9). PPO hydrophobic core carries hydrophobic drugs, and the PEO shells take hydrophilic drugs.<sup>220,221</sup> Adjusting the composition, molecular weight, and concentration of the polymer-building units favors the synthesis of various pluronic products, such as F-68, F-127, P-103, and P-105.<sup>222–224</sup> Pluronic copolymers are versatile for chemical modification because they possess end hydroxyl groups.<sup>225,226</sup> To address the limitations of pluronic hydrogels, such as low stability under physiological conditions, fast dissolution rate, low mechanical strength, and low biodegradability, interactions with polymers exhibiting greater stability and biocompatibility have been explored.<sup>144,227,228</sup> One alternative approach involves the chemical cross-linking of hydrogels to enhance their stability. Chemical crosslinking also increases the drug loading and retention times of pluronic hydrogels.<sup>229,230</sup> Another approach is the conjugation of natural or synthetic chemical molecules, such as proteins, carbohydrates, and nucleotide bases, with pluronic to form more stable multiblock copolymers.<sup>231–233</sup>

Among the various Pluronic-based hydrogels, F127 has been comprehensively applied in anti-cancer drug delivery research.

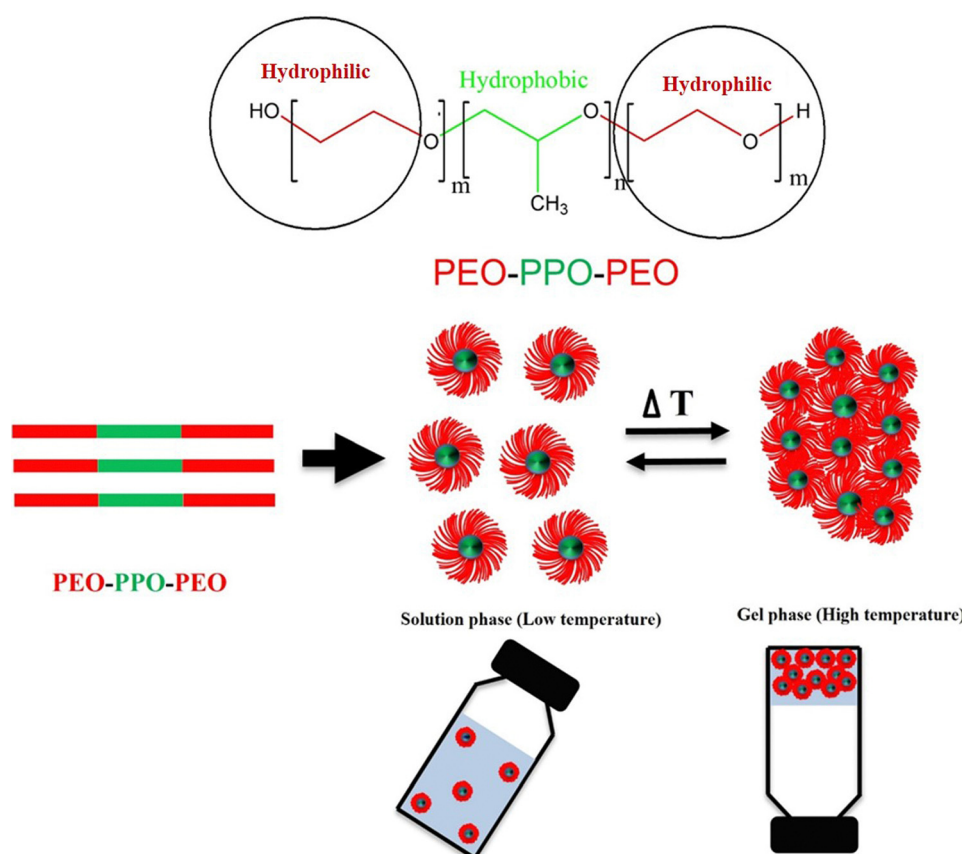
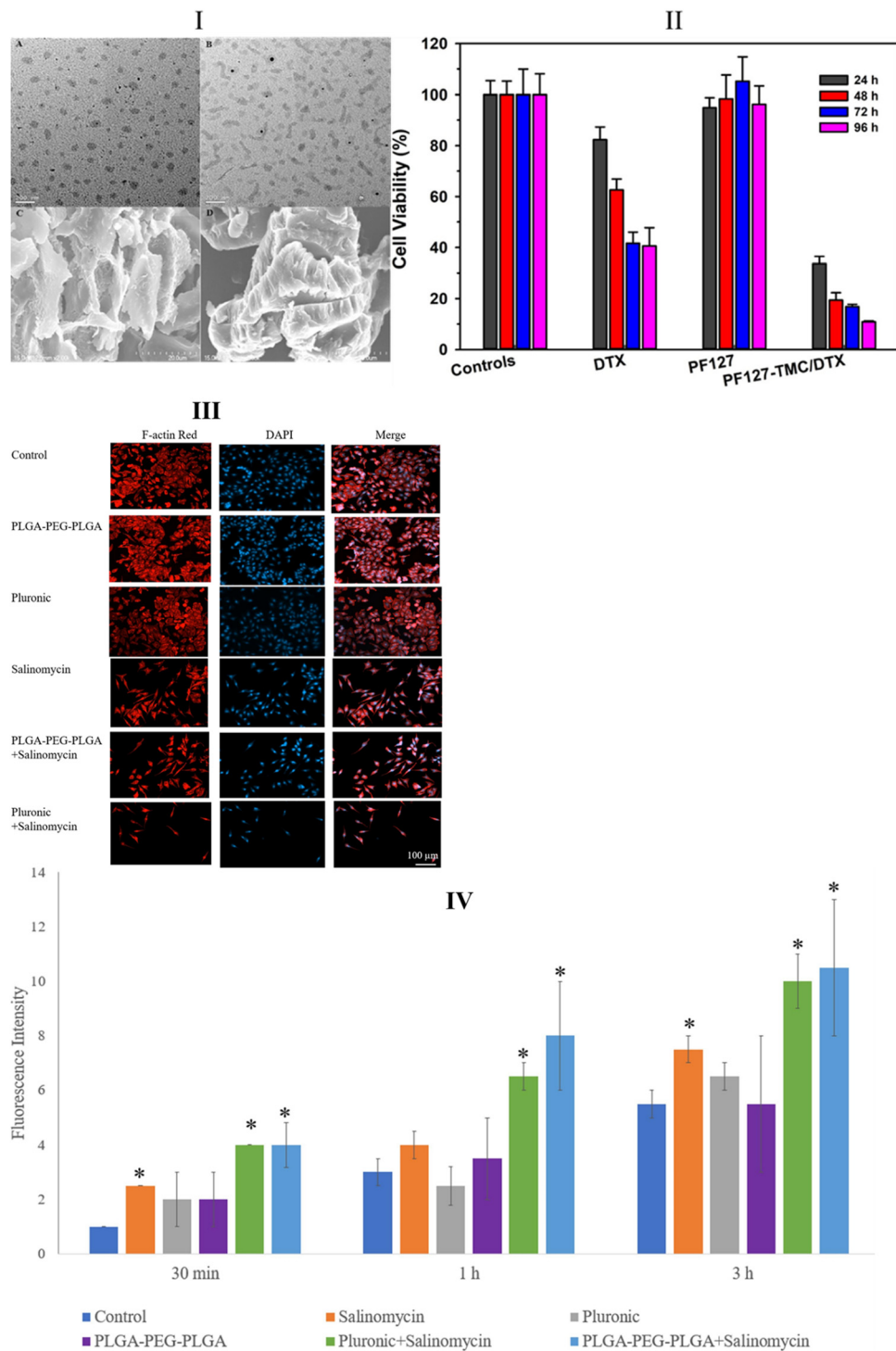


Fig. 9 Diagrammatic representation of the temperature-dependent sol–gel transition of F127 hydrogels.



Blending F127 with chitosan, alginate, heparin, hyaluronic acid, and cellulose derivatives enables sustained and diffusion-resistant anti-cancer drug delivery, addressing the rapid disintegration of F127.<sup>234,235</sup> Moreover, the mechanical strength of F127 hydrogels



**Fig. 10** Transmission electron microscopy (TEM) images of PF127-TMC/DTX gel (I-A) and PF127/DTX gel (I-B); scanning electron microscopy (SEM) images of PF127-TMC/DTX gel with a more distinct and regular porosity structure (I-C) and PF127/DTX gel (I-D). Cytotoxicity tests were performed on U87MG cells with controls, docetaxel, docetaxel loaded on PF127, and docetaxel loaded on PF127-TMC (II). Fluorescence microscopy images of U251 cells after treatment with salinomycin, F127, and PLGA-PEG-PLGA. Red fluorescence represents Alexa Fluor at 488 phalloidin-stained F-actin, and blue fluorescence reveals DAPI-stained cell nuclei (III). Reactive oxygen species (ROS) levels in U87MG cells treated with salinomycin and salinomycin-loaded hydrogels at three different time points (IV). Images (I) and (II) are reprinted from ref. 245, and images (III) and (IV) are reprinted from ref. 246 with permission from the publishers and (order license ID 1338403-1, 27 March 2023, respectively).



Table 2 Selected pluronic-based thermally sensitive hydrogels and their potential as drug carriers for various cancer types



Table 2 (continued)

Name of the pluronic hydrogel	Structure of the hydrogel	Anti-cancer drug carried by the hydrogel	Cancer type	Earned benefits of copolymerization	Advantages of using the hydrogel	Ref.
Heparin-poloxamer-407 nano gel		Doxorubicin (DOX)	S-180 (sarcoma) cells	✓ Enhanced mechanical strength and stability	✓ High drug entrapment efficiency ✓ Suspended and controlled drug release with best anti-tumor efficacy <i>in vitro</i> and <i>in vivo</i>	253
Pluronic hydrogels		Codeelivery of DOX and 5-fluoro uracil (FU)	B16F (melanoma) cells	✓ Enhanced prolonged release of the drug and anti-cancer activity	✓ Dominant tumor growth inhibition ✓ Maintained drug distribution only in the target tumor cells ✓ Reduced plasma concentration of the drugs	254
Poloxamer 407 hydrogel		Holmium-containing bioactive glasses	MG-63 bone cancer cells	✓ No copolymerization implemented	✓ Enhanced pre-osteoblastic cell growth ✓ Better killing of osteosarcoma cells	255

can be enhanced by incorporating crosslinker salts, such as sodium phosphate and sodium chloride.<sup>236</sup> Generally, due to its improved stability, F127 hydrogel holds significant importance within the Pluronic family for anti-cancer drug delivery applications.<sup>237</sup>

**4.3.2.1. Thermal-sensitive pluronic-based hydrogels used in local drug delivery of cancer.** Despite the fast disintegration rate and low mechanical strength of Pluronic hydrogels posing challenges to anti-cancer drug delivery, scientists still favor their use by developing methods to address these issues.<sup>231</sup> This preference stems from the inherent adjustability of Pluronic structures, which enables efficient hydrophobic drug delivery.<sup>238,239</sup> Moreover, enhancing the strength and stability of Pluronic hydrogels can be achieved by copolymerizing their hydroxyl end group with more stable side-chain polymers.<sup>240</sup> For instance, the binding of polycaprolactone, hydroxy propyl methylcellulose, and methylcellulose to the hydroxyl end of Pluronic prolongs the drug release process by increasing the stability of the polymer.<sup>241</sup> A recent study demonstrated that a highly viscous liposomal copolymer hydrogel produced from F127 demonstrated extended drug release duration and zero-order kinetics for delivering the antineoplastic agent paclitaxel to human oral cancer KB cells.<sup>239</sup> Glioblastoma is notorious for its low therapeutic response owing to the limited systemic drug delivery across the BBB.<sup>242,243</sup> Local drug delivery using Pluronic copolymer hydrogels offers a promising solution to challenges associated with the BBB.<sup>244</sup> The *N,N,N*-tri methyl chitosan (TMC)-embedded F127 copolymer hydrogel has demonstrated promising docetaxel delivery to U87MG cells.<sup>245</sup> Scanning electron microscopy (SEM) and transmission electron microscopy (TEM) images of the thermally sensitive TMC-F127 hydrogels revealed a porous network (Fig. 10I). In this study, the TMC-F127 hydrogel-delivered docetaxel outperformed both the free drug and the drug delivered with F127 gels in killing U87MG cells, as confirmed by the MTT assay (Fig. 10II). In another study, the PF127 hydrogel exhibited 100% efficacy as a chemotherapeutic agent for salinomycin release, suppressing proliferation, inducing apoptosis, and increasing intracellular ROS in mouse xenografted subcutaneous U251 brain tumors.<sup>246</sup> The study utilized PLGA-PEG-PLGA and PEO-PPO-PEO (PF127) hydrogels to deliver salinomycin. According to fluorescent microscopy images (Fig. 10III) and intracellular peroxide-dependent oxidation of 2',7'-dichlorofluorescein diacetate (DCFDA), PF127-salinomycin demonstrated dominance in killing U251 cells while producing comparable ROS levels with PLGA-PEG-PLGA-salinomycin polymers (Fig. 10IV). Strategically designed, thermally sensitive Pluronic-based copolymer hydrogels have been utilized to deliver various anti-cancer drugs *in vitro* and *in vivo* for treating different cancer types (Table 2).

**4.3.3. Poly ethylene glycol (PEG) based hydrogels.** PEG is a widely used petroleum-derived, thermally sensitive hydroxy poly-ether approved by the FDA for pharmacological applications, including drug delivery.<sup>256</sup> PEG is also known as polyethylene oxide (PEO) or polyoxyethylene (POE), depending on its molecular weight.<sup>257,258</sup> PEG polymers possess a lower molecular weight than PEO polymers, with a molecular weight greater than 20 000.

The ethylene oxide polymer of PEG consists of a repeating unit of  $-(O-CH_2-CH_2)$ .<sup>259</sup> PEG can be synthesized through anionic polymerization of ethylene oxide with hydroxyl initiators, such as water and epoxy ethane.<sup>260</sup> Hydrophilic low-molecular-weight PEG exhibits low antigenicity or immunogenicity and can be rapidly eliminated through the kidneys.<sup>261,262</sup> When combined with hydrophobic components like peptides, the 3D hydrophilic crosslinked polymer of PEG displays anti-cancer drug delivery potential, specifically maintaining drug stability and release for up to one month.<sup>263,264</sup> In PEG-based hydrogel structures, covalent PEG grafting with other polymers, known as PEGylation, enhances stability and biocompatibility. Abuchowski and Davis first proposed PEGylation in the late 1970s, with the first clinical success achieved in 1990 with the delivery of adagin for immune deficiency diseases.<sup>265</sup> PEGylation transforms hazardous hydrophobic compounds, which can pass through cell membranes and enter cells, into non-toxic hydrophilic components.<sup>266</sup> This detoxification occurs because liver enzymes can interact with the hydrophilic PEG portion and facilitate its excretion *via* the kidneys.<sup>267</sup> The PEGylation of hydrophobic polymers like poly(lactic-co-glycolic) acid (PLGA) and polycaprolactone has recently gained research interest due to their superior biodegradability and biocompatibility compared to other thermally sensitive hydrogels.<sup>268,269</sup> These amphiphilic copolymers exhibit a unique micellar arrangement and aggregate upon temperature changes.<sup>270</sup> The widely used poly ethylene glycol-poly propylene glycol-poly ethylene glycol (PEG-PPG-PEG) tri-block copolymer features a hydrophilic PEG layer and a hydrophobic PPG core connected through an ester linkage.<sup>271</sup> Small micelles with hydrophobic PPG and hydrophilic PEG shells form at lower temperatures, maintaining the mixture in a solution state. However, upon exposure to higher temperatures, the micelles aggregate, increase in size, and form gels due to the dehydration of the PEG hydrophilic shell (Fig. 11).<sup>272,273</sup> This thermogelling

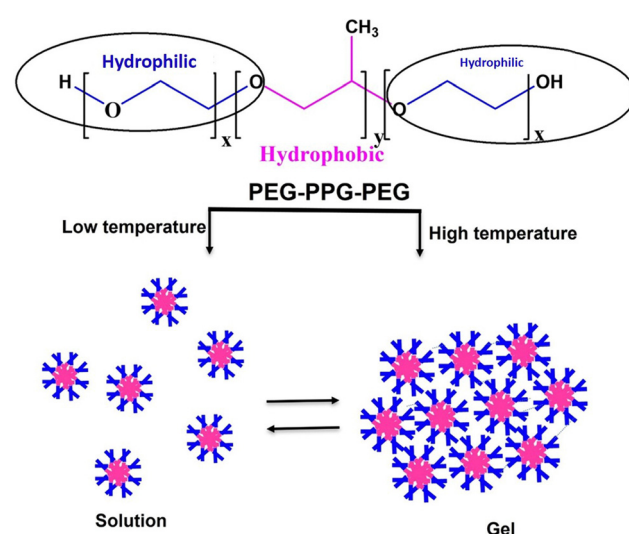


Fig. 11 Diagrammatic representation of temperature-dependent sol-gel transition of poly ethylene glycol-poly propylene glycol-poly ethylene glycol (PEG-PPG-PEG) hydrogels.



property balances the hydrophilic and hydrophobic moieties of the micelles.<sup>274</sup> Besides the balance of moieties, temperature-based gelling of PEG hydrogels is regulated by factors, such as the polyester block composition and molecular weight distribution.<sup>275</sup> Furthermore, the drug release rate from PEG copolymer hydrogels depends on the synthesis method, cross-linking density, drug solubility, and molecular weight of the PEO chains.<sup>276</sup> PEG-based hydrogels remain in blood circulation longer in a typical injectable delivery system, allowing for the complete release of the drug to the target site. In contrast, drug injection alone results in rapid drug entry into target cells, leading to drug component breakdown before achieving the desired efficacy.<sup>277</sup> The thickness of PEG in copolymer hydrogels plays a crucial role in preventing serum protein adsorption into hydrogel segments, and its effectiveness is influenced by the

molecular weight, conformation, and density.<sup>278,279</sup> Therefore, the PEG molar ratio directly affects the stability and protection of drugs encapsulated in PEG-based hydrogels.<sup>265</sup>

**4.3.3.1. Thermal sensitive PEG based hydrogels used in local drug delivery of cancer.** The elastic properties and favorable safety profile of PEG copolymer hydrogels allow for facile loading and distribution of anti-cancer drugs to local areas and preparing injectable hydrogel solution forms.<sup>191</sup> Furthermore, PEG-based hydrogels with diverse morphologies can effectively release drugs at physiological temperature (37 °C) and tumoral pH (5.5).<sup>280</sup> DOX can be loaded onto PEG-based hydrogels by mixing the solutions at low temperatures, efficiently inhibiting the topoisomerase II enzymes of A549 lung cancer cells and suppressing proliferation at the gene

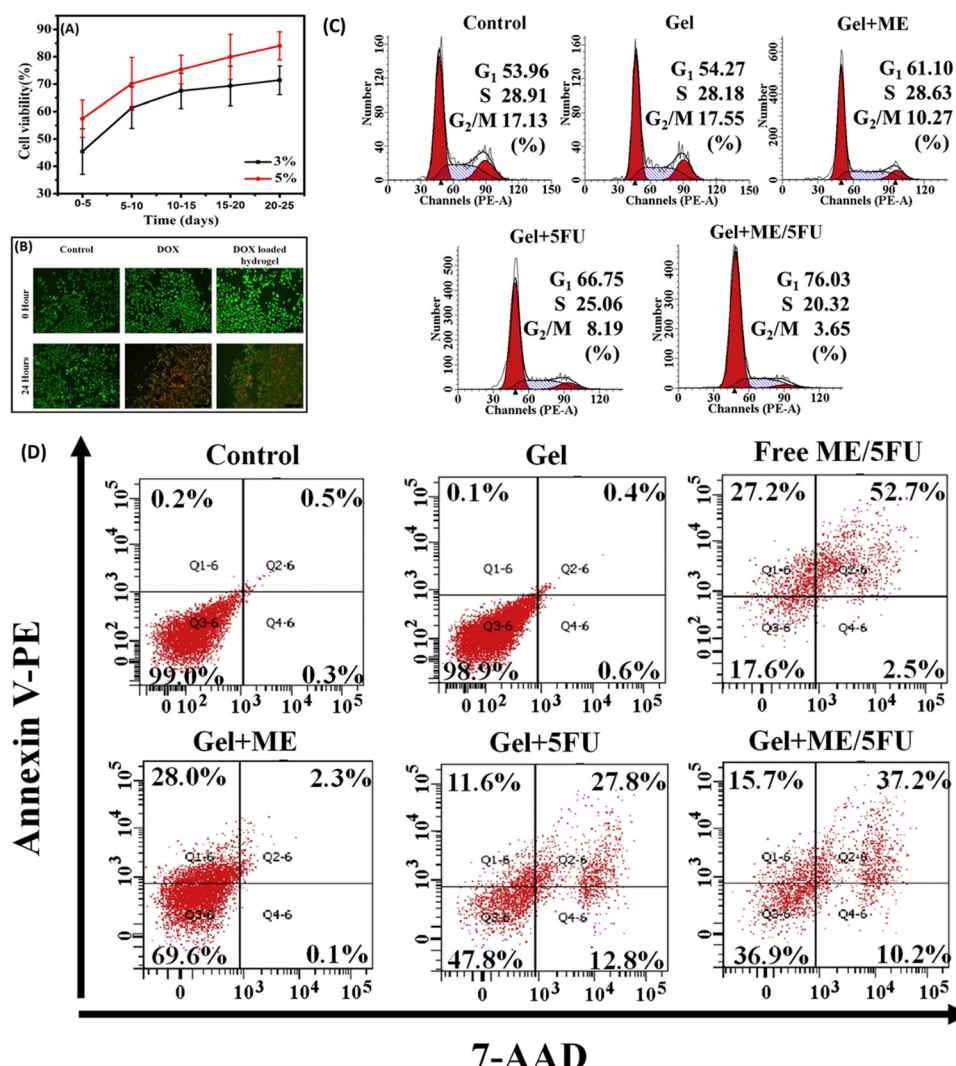


**Fig. 12** (A) Viability of A549 cells after treatment with 3 and 5% PEG-based hydrogel for 25 d and (B) fluorescent microscopy images of control, DOX, and DOX-loaded PEG-based hydrogel-treated A549 cells, demonstrating a viability change after 24 h of treatment. (C) Cell cycle distribution of C26 cells before and after treatment with PEG-based hydrogel, Metformin, PEG-based hydrogel plus metformin, PEG-based hydrogel plus 5-fluorouracil, and PEG-based hydrogel plus metformin and 5-fluorouracil. (D) Annexin V-PE/7-AAD stained flow cytometric analysis of apoptosis induced after treatment with PEG-based hydrogel, free metformin, and 5-fluorouracil, PEG-based hydrogel plus metformin, PEG-based hydrogel plus 5-fluorouracil, and PEG-based hydrogel plus metformin and 5-fluorouracil. Images (A) and (B) adapted from ref. 281, (C) and (D) reprinted from ref. 282 with permission from the publisher (order license ID: 1338413-1, 27 March 2023).



transcription stage. Additionally, cell viability studies revealed that treatment with the DOX-loaded PEG copolymer hydrogel resulted in higher cytotoxicity in A549 cancer cells for up to 25 d compared to DOX alone (Fig. 12A).<sup>281</sup> In another study, local co-delivery of metformin and 5-fluorouracil using a hydrogel synthesized *via* a Schiff base reaction between 4-arm PEG and 4-arm-PEG-*b*-poly(*l*-lysine) demonstrated improved synergistic antitumor efficacy and increased apoptosis induction in C26 colon carcinoma cells *in vitro* and *in vivo*.<sup>282</sup> Co delivery of metformin and 5-fluorouracil can decrease cancer cell proliferation during the G1 phase of the cell cycle.<sup>283,284</sup> Particularly, 5-fluorouracil can suppress tumor cell development in the G1/S phase of the cell cycle and trigger p53-dependent apoptosis.<sup>285</sup> Furthermore, compared to treatment with the hydrogel and dual drugs individually, co-treatment with the PEG-based hydrogel demonstrated the highest percentage of C26 cell cycle arrest at the G1 phase (Fig. 12C). Numerous drug delivery studies have been conducted on PEG copolymer hydrogels. The delivery and effects of anti-cancer drugs for various cancer types using PEG-based hydrogels, as well as the benefits attained through the copolymerization of PEG, are discussed in detail (Table 3).

## 5. Reactive oxygen species (ROS) responsive hydrogels

### 5.1. Why ROS sensitive hydrogels are used for anti-cancer drug delivery?

Moderate levels of ROS, which are endogenous metabolic byproducts generated in the mitochondria, are essential for proper cell signaling pathways.<sup>295</sup> At low concentrations, ROS effectively regulate cell activity by acting as immune system agents, cell signaling regulators, protein function modulators, and mediators of cell development and apoptosis.<sup>296,297</sup> These beneficial activities are primarily performed by ROS through the reversible oxidation of thiol groups in structural or functional proteins, leading to modifications in protein structure and function.<sup>298</sup> However, continuous ROS production must be accompanied by the disposal of metabolic pathways catalyzed by superoxide dismutase, peroxidase, and catalase enzymes.<sup>299,300</sup> Abnormal or excessive ROS accumulation can trigger persistent oxidative stress, resulting in damage and structural alterations to vital macromolecules like membrane proteins, lipids, and DNA.<sup>301</sup> This disruption to the metabolic balance leads to various diseases, including cancer, cardiovascular disease, arthritis, diabetes, and neurological disorders.<sup>302,303</sup>

The tumor microenvironment differs from that of normal cells in terms of physiological conditions such as pH, temperature, enzyme levels, and ionic strength.<sup>304</sup> These differences promote tumor cell growth and proliferation while inhibiting the life cycle of healthy cells.<sup>305,306</sup> An abnormal increase in ROS may be at the forefront of these alterations.<sup>307</sup> Elevated ROS levels in cells reduce oxygen (O) and expedite the excessive formation of products, such as hydrogen peroxide ( $H_2O_2$ ), superoxide, hydroxyl radicals, and peroxynitrite, causing

oxidative stress.<sup>121,308</sup> Under most physiological circumstances, the detoxification of ROS generated as metabolic products, is performed by an intracellular oxidation-reduction balance system.<sup>309</sup> However, the tumor microenvironment disrupts this balance system by inhibiting key enzymes that catalyze detoxification or by producing an excessive amount of ROS that surpasses the detoxifying capacity of the balance system's enzymes.<sup>310,311</sup> For instance, glucose-6-phosphate dehydrogenase (G6PD) is a crucial regulator of the hexose phosphate shunt route and indirectly reduces oxidized glutathione (GSSG) in red blood cells lacking mature mitochondria.<sup>312,313</sup> Under normal conditions, reduced nicotine adenine di nucleotide phosphate (NADPH), a product of G6PD, supplies H to GSSG, which then converts into reduced glutathione (GSH) (Fig. 13). Subsequently, GSH donates H to the glutathione peroxidase-catalyzed reaction, neutralizing  $H_2O_2$  into water (Fig. 12).<sup>314,315</sup> This implies that  $H_2O_2$  detoxification is associated with the formation of reduced GSH, which serves as a H ion carrier during detoxification.<sup>316</sup> Therefore,  $H_2O_2$  produced in blood cells cannot be neutralized when G6PD is defective (resulting in no production of NADPH) (Fig. 13).<sup>317,318</sup> Increased levels of  $H_2O_2$  in red blood cells cause oxidative stress, associated with DNA damage and mutations that initiate the proliferation of leukemia cells.<sup>319</sup> Therefore, altered activity of G6PD, glutathione reductase, and glutathione peroxidase contributes to the emergence and uncontrolled proliferation of leukemic cells.<sup>320,321</sup> Elevated ROS production promotes ROS-induced mitochondrial dysfunction, activating MMPs that initiate the proliferation of various cancer types.<sup>322</sup> Overproduction of ROS in normal breast cells can induce human breast carcinomas by damaging genes regulating standard growth patterns through ROS-mediated activation of mitogen-activated protein kinases.<sup>323,324</sup> This induction may also be associated with increased expression of NADPH oxidases, causing elevated levels of  $H_2O_2$ , followed by aggressive breast tumor initiation.<sup>325</sup> Uncontrolled ROS levels in normal cells can also induce hepatocellular carcinoma,<sup>326</sup> cervical cancer,<sup>327</sup> and lung cancer.<sup>328</sup> In contrast, deliberately increasing ROS levels in cancer cells can serve as a treatment, as it induces programmed cancer cell death through apoptosis and related autophagy mechanisms.<sup>329,330</sup>  $H_2O_2$  does not directly cause DNA damage during cancer cells.<sup>331</sup> However, high  $H_2O_2$  concentrations activate the formation of OH radical ions through the Fenton reaction (involving  $H_2O_2$  and  $Fe^{2+}/Cu^{+}$ ), which can then react with DNA to activate oncogenes, such as K-Ras.<sup>332,333</sup> Generally, an impaired antioxidation system and disrupted homeostasis in the tumor microenvironment result in increased ROS levels in this region.<sup>334</sup> This has led to the development of ROS-sensitive hydrogels that can carry and release anti-cancer drugs upon exposure to an enhanced ROS environment.<sup>121</sup>

### 5.2. Possible ROS sensitive groups to form hydrogels

The application of ROS-responsive hydrogels in anti-cancer drug delivery is still in its infancy, but it has recently garnered increased interest.<sup>335</sup> Consequently, the development of anti-



Table 3 Selected PEG-based thermally sensitive hydrogels and their potential as drug carriers for various cancer types

Name of the PEG hydrogel	Structure of the hydrogel	Anti-cancer drug carried by the hydrogel	Cancer type	Earned benefits of copolymerization	Advantages of using the hydrogel	Ref.
$\text{CO}_2\text{H-PDLA-PEG-PDLA-CO}_2\text{H}/\text{NH}_2$ -PDLA-PEG-PDLA-NH <sub>2</sub> (carboxyl end and amino end modified poly( $\text{D,L-}$ lactide)-poly(ethylene glycol)-poly( $\text{D,L-}$ lactide copolymer))		DMXAA and doxorubicin	HeLa (cervical cancer cells)	✓ Enhanced mechanical stability and drug loading efficiency	✓ Capacity of increasing tumor suppression and reducing tumoral micro vessel density	272
Sa-PDLA-PEG-PDLA-SA (HO <sub>2</sub> -CPP-COO <sub>2</sub> H)		CMHA-PDLA-PEG-PDLA-CMHA (NH <sub>2</sub> -PPP-NH <sub>2</sub> )	Bevacizumab and doxorubicin	✓ Enhanced biodegradability and mechanical strength	✓ Improved drug releasing capacity at tumoral PH (6.5)	286
Poly( $\text{D,L-}$ lactide)-poly(ethylene glycol)-poly( $\text{D,L-}$ lactide) (PDLA-PEG-PDLA)		Oxidized xanthan	A549 (lung cancer cells)	✓ Enhanced biodegradability and mechanical strength associated with self-healing capacity during a breakdown	✓ Highest DOX releasing efficiency at tumoral PH (5.5)	287
Xanthan PEG hydrogels		Hydrazone linkage	Doxorubicin	✓ Improved gelation capacity due to enhanced storage modulus value	✓ Rapid release of bevacizumab followed with long term release of doxorubicin	288
8-arm PEG hydrazine		PEG	Human orthotopic breast tumors (in vitro)	✓ Stabilized hydrogel structure with defined mesh size	✓ Enhanced anti-tumoral effect include inhibition of tumor growth and metastasis	289
$\text{X=SO}_3\text{H}\cdot\text{H}$		Therapeutic T-lymphocytes (immunotherapy)	Glioblastoma	✓ Optimal pore size and enhanced stability	✓ Better effectiveness on killing glioblastoma cells	290



Table 3 (continued)

Name of the PEG hydrogel	Structure of the hydrogel	Anti-cancer drug carried by the hydrogel	Cancer type	Earned benefits of copolymerization	Advantages of using the hydrogel	Ref.
Poly(ethylene glycol) diacrylate (PEGDA) — and thiolated gelatin poly(ethylene glycol) (Gel-PEG-Cys) cross-linked hydrogels		MI macrophages	Human hepatocellular carcinoma ( <i>in vitro</i> and <i>in vivo</i> )	✓ Mechanical strength and associated release of the M1 macrophages	✓ Enhanced tumor regression with followed induction of apoptosis	290
Poly(ethylene glycol) methyl ether methacrylate and dimethacrylate hydrogel					✓ Tunability and strength for thermal resistance	291
Poly( $\epsilon$ -caprolactone- <i>co</i> -lactide)- <i>b</i> -poly(ethylene glycol)- <i>b</i> -poly( $\epsilon$ -caprolactone- <i>co</i> -lactide) hydrogel		Gemcitabine	Pank-1 cells (pancreatic cancer cell, <i>in vivo</i> )	✓ Better mechanical stability and strength	✓ Enhanced half-life of the drug with reduced cytotoxicity and therapeutic efficacy	292
Poly[ $(\alpha$ -benzyl carboxylate- <i>e</i> -caprolactone)- <i>co</i> - $(\alpha$ -carboxyl- <i>e</i> -caprolactone]- <i>b</i> -PEG- <i>b</i> [ $(\alpha$ -benzyl carboxylate- <i>e</i> -caprolactone)- <i>co</i> - $(\alpha$ -carboxyl- <i>e</i> -caprolactone)] (PCBCL- <i>b</i> -PEG- <i>b</i> -PCBCL)		Silibinin	BT4-F10 cells (melanoma, <i>in vitro</i> and <i>in vivo</i> )	✓ Subcutaneous stability, enhanced loading and release of silibinin	✓ Highest cytotoxicity of B16-F10 cells due to improved inhibition of proliferation, cell cycle arrest, and induction of apoptosis	293
Poly( $\epsilon$ -lactide- <i>co</i> -glycolide)-poly(ethylene glycol)-poly(lactide- <i>co</i> -glycolide) (PLGA-PEG-PLGA)		Doxorubicin and cisplatin	Human osteosarcoma xenografts	✓ Mechanical strength and stability	✓ Loading capacity of co-drugs, highest anti-proliferative activity and regulation of apoptosis related gene expression	294

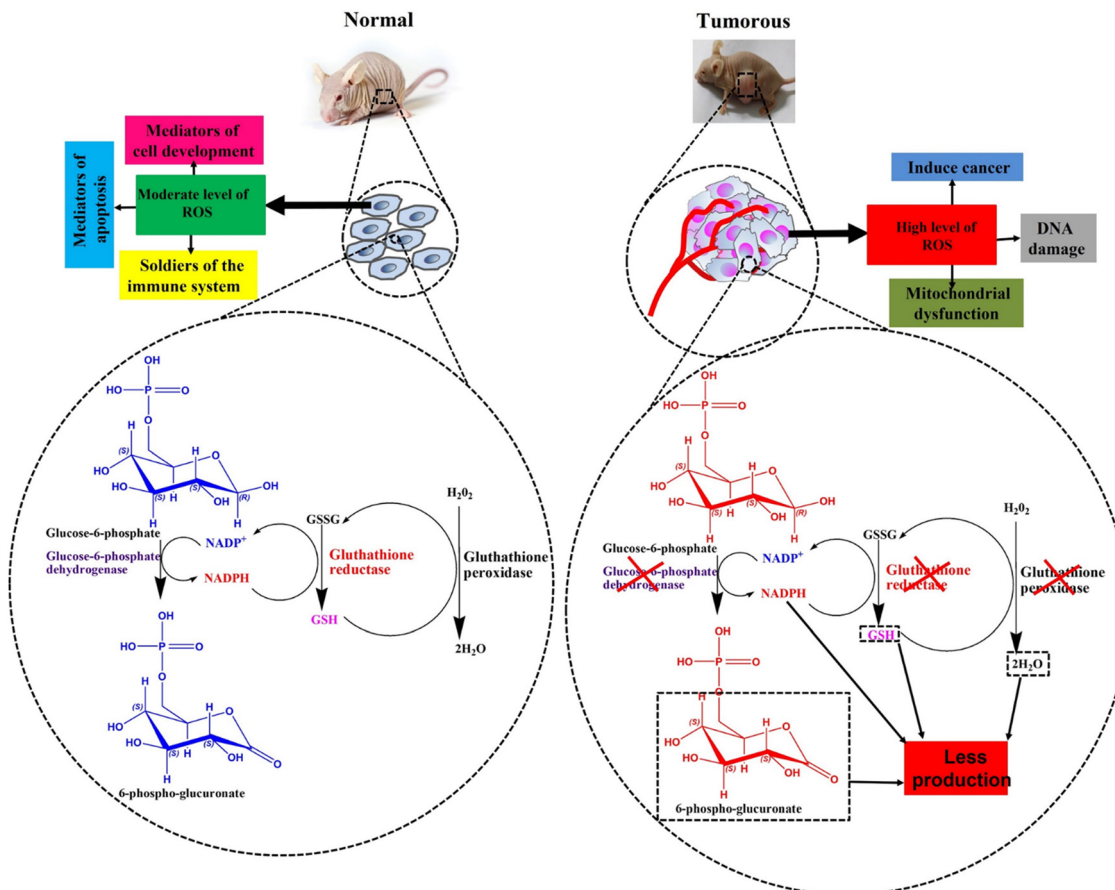


**Fig. 13** Diagrammatic view of glucose-6-phosphate dehydrogenase reaction and the levels of glutathione (GSH), nicotinamide adenine dinucleotide phosphate (NADPH), and hydrogen peroxide ( $H_2O_2$ ) in normal and tumorous cells.

cancer drug delivery systems based on ROS-responsive hydrogels seems to be a promising future direction. Numerous studies have explored the use of ROS-responsive nano capsules for drug delivery.<sup>336</sup> However, further research is needed to fully understand the potential of ROS-responsive hydrogels in anti-cancer drug delivery applications.<sup>33,337</sup> Therefore, we can gain valuable insights into the fabrication of ROS-responsive hydrogels by examining existing literature and employing established methods for creating ROS-responsive nano carriers.

During the copolymerization process, a widely used technique for creating ROS-responsive hydrogels, ROS-responsive chemical compounds can be integrated into the hydrogel's backbone.<sup>121,338</sup> Since the majority of these compounds are hydrophobic, they can serve as hydrophobic components or be conjugated with a hydrophobic moiety in an amphiphilic copolymer during synthesis.<sup>339</sup> Structures containing selenium (Se), tellurium (Te), aryl boronic ester, poly(L-methionine), poly(L-proline), and disulfide are ROS-responsive groups that can be employed in the fabrication of ROS-responsive hydrogels.<sup>340,341</sup> These molecules may undergo an ROS-induced non-cleavable hydrophobic-to-hydrophilic transition or ROS-induced structural cleavage, allowing for the release of the encapsulated drug molecules.<sup>338,340–342</sup> The hydrophobic-hydrophilic transition occurs when an O atom forms a covalent

bond with surrounding molecules. This process involves the ROS-induced oxidation of chalcogen elements, such as sulfur (S), Se, and Te, altering their valence from +2 to +4 or +6 (Fig. 14A). In contrast, the reaction of ROS with aryl boronic acid/ester, thioether, thioketal, and proline oligomers facilitates the cleavage of polymers or hydrogels composed of these groups.<sup>338</sup>

S-containing hydrogels can be synthesized using S-containing amino acids such as cysteine, methionine, homocysteine, and taurine.<sup>343</sup> As S is abundant in nature in these amino acids, its polymer structure is less toxic and biocompatible.<sup>344</sup> Disulfide bonds are commonly used in ROS-responsive drug delivery systems. Incorporating disulfide bonds, which are temperature-sensitive, during synthesis can produce thermally sensitive gels.<sup>345</sup> The first S-containing triblock copolymer vesicle (PEG-polypropylene sulfide-PEG) capable of undergoing a hydrophobic-to-hydrophilic transition upon exposure to an  $H_2O_2$ -rich environment was synthesized in 2004.<sup>346,347</sup> Drug loading into these vesicles can be achieved either in amphiphilic ROS-responsive micelles or in the ROS-responsive backbone of the polymer [315].<sup>348</sup> Other well-known S-containing polymers and thioethers can be synthesized through transfer polymerization, ring-opening polymerization, and step-growth polymerization.<sup>349</sup> Thioethers, which are also



responsive to high ROS environments, can react with  $\text{H}_2\text{O}_2$  and generate a solubility shift, causing carrier decomposition and subsequent release of the loaded drug.<sup>348,350</sup> Due to its inability to oxidize thioethers under normal physiological conditions, superoxide dismutase contributes to the degradation of thioethers by producing  $\text{H}_2\text{O}_2$ .<sup>341</sup> Polypropylene sulfide is a widely used polymer in nanovesicle synthesis. It possesses temperature-responsive gelation properties and can transform into hydrophilic components when exposed to high ROS environments.<sup>351</sup> These characteristics make polypropylene sulfide an excellent component for the development of thermal and ROS-responsive hydrogels in anti-cancer drug delivery.<sup>352</sup> Thioketals, S-containing ROS-sensitive groups, are suitable for designing ROS-responsive hydrogels. The thioketal bond is sensitive to high ROS environments, undergoing a reaction that yields acetone, while the other two S-containing moieties result in the breakdown of the linkage (Fig. 14B).<sup>353</sup> Xia and Shim synthesized ROS-responsive polymers containing thioketal groups and successfully delivered specific DNA sequences.<sup>354</sup>

Se-containing polymers, synthesized through step-growth polymerization, play a crucial role in neutralizing peroxides in cells by enhancing the catalytic activity of glutathione peroxidase.<sup>355–357</sup> Additionally, Se ions have demonstrated the ability to kill cancer cells.<sup>358</sup> Di selenium-containing polymers are ideal for use as components in ROS-responsive hydrogels for targeted anti-cancer drug delivery.<sup>191,359</sup> In the presence of high ROS concentrations, Se-containing polymers can oxidize to selenoxide, then reduce to selenones, leading to a hydrophobic-to-

hydrophilic phase transition and bond cleavage, ultimately releasing the drug.<sup>360</sup> Researchers have successfully synthesized ROS-sensitive supramolecular hydrogels composed of peptide amphiphiles and selenide copolymers, which release naproxen in higher ROS environments.<sup>361</sup>

Te-containing polymers, synthesized similarly to Se polymers through step-growth polymerization, exhibit ultra-sensitive ROS-responsive potential (100  $\mu\text{m}$ ) compared to other groups. However, Te, a member of the chalcogen family, is known to have toxic effects on cells.<sup>362</sup> As a result, enhancing biocompatibility is a primary objective when preparing Te-containing polymers.<sup>362</sup> Wang *et al.* reported the synthesis of a nanocarrier comprised of a copolymer of Te-containing molecules and phospholipids, which demonstrated both Te ROS responsiveness and phospholipid biocompatibility, potentially addressing the biocompatibility issue.<sup>363</sup> Other studies have also highlighted the improved biocompatibility of Te-containing hydrogels for anti-cancer drug delivery. For instance, Te-containing nanocarriers capable of coordinating chemotherapy, photodynamic therapy, and photothermal therapy have been synthesized with reduced toxicity and enhanced biocompatibility. The PEG-PUTE-PEG copolymer allowed for controlled and prolonged release of cisplatin while incorporating the capacity for near-infrared light irradiation.<sup>364</sup> In general, future designs of Te-incorporated hydrogels should focus on increasing biocompatibility while maintaining ROS sensitivity.

Other ROS-sensitive polymers, such as PBE or ABE, can be synthesized through a stepwise polymerization reaction using

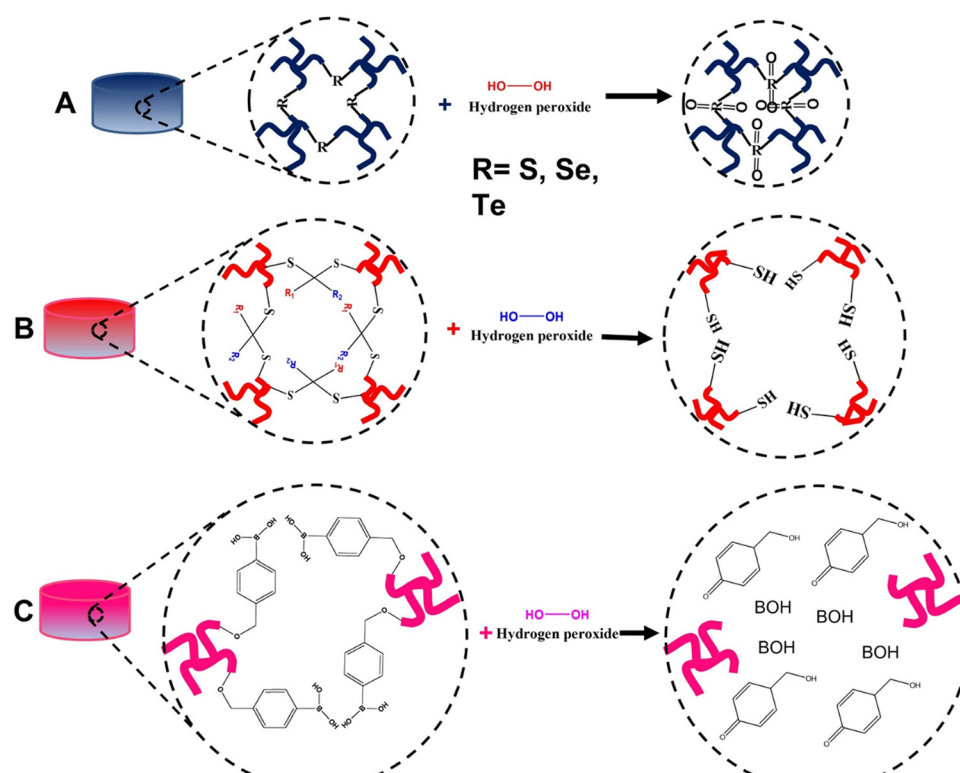


Fig. 14 Diagrams of hydrogel structures with possible  $\text{H}_2\text{O}_2$  oxidation reactions (A) sulfur, selenium and tellurium, (B) thioketal, and (C) boronic acid.



PBE or ABE monomers. These polymers are selectively oxidized by  $H_2O_2$  to produce phenol or aryl and boronic acid groups as products (Fig. 14C).<sup>342,365</sup> This reaction involves the ROS-induced oxidation of the carbon–boron link, forming phenol borate, which is then hydrolyzed to produce boronic acid and phenol. Similarly, aryl boronic esters undergo consecutive oxidation and hydrolysis to yield phenol and aryl boronic acids as final products.<sup>366</sup> Instead of serving as a hydrophobic component of the carrier in drug carrier polymer construction, PBE forms a weak  $\pi$ – $\pi$  interaction with the drug to enhance its stability.<sup>367</sup>

Proline can also undergo ROS-mediated oxidation to form tertiary amine bonds with relatively strong oxidation properties.<sup>368</sup> Due to their slow degradation rate, proline oligomers are preferable candidates for synthesizing drug carriers that allow for prolonged release.<sup>369</sup> Their complete degradation can take weeks, in contrast to other polymers that degrade in hours or days.<sup>360</sup> Furthermore, since proline is a natural component, incorporating it into copolymer carriers can enhance their biocompatibility.<sup>54</sup>

The final ROS-sensitive polymers discussed here are those containing ferrocene. Atom transfer radical reactions can be employed to synthesize these polymers.<sup>370,371</sup> Ferrocene-containing polymers belong to an organometallic chemical family with two cyclopentadienyl rings on opposite sides of a central iron atom.<sup>372</sup> These polymers are more stable and can be effectively synthesized with reversible redox activities.<sup>373</sup> Similar to other ROS-responsive groups, ferrocene-containing polymers constitute the hydrophobic components of amphiphilic drug carriers.<sup>374</sup> Upon exposure to a high ROS environment, the hydrophobic ferrocene group rapidly oxidizes to hydrophilic ferricinium.<sup>375,376</sup> Due to their phase transition capability, these compounds are suitable for ROS-triggered drug release. Future hydrogel designs should consider incorporating these groups.<sup>121,191</sup>

**5.2.1. ROS-sensitive hydrogels used in local drug delivery for cancer treatment.** As mentioned in the previous section, the use of ROS-sensitive hydrogels for anti-cancer drug delivery is in the early stages of development. In this section, we discuss some research findings on this topic. Chao Wang *et al.* reported an ROS-sensitive hydrogel scaffold synthesized from a combination of  $N_1,N_1,N_3,N_3$ -tetramethyl propane-1,3-diamine, excess 4-(bromomethyl)phenyl boronic acid (TSPBA), and poly(vinyl alcohol) (PVA). The hydrogel promoted immunogenic types of B16F10 (melanoma tumor) and 4T1 (breast tumor) *in vivo* (mouse models) *via* gemcitabine delivery, increasing the anti-tumor response through the release of anti-PD-L1 blocking antibody.<sup>377</sup> Thus, the PVA-TSPBA hydrogel reduced the side effects associated with immune checkpoint and PD-1/PD-L1 pathway inhibitors. Three different groups of mouse models were used to induce B16F10 tumors (untreated, hydrogel-treated, and gemcitabine-hydrogel-treated). The highest PD-L1 expression was observed in cancer cells, dendritic cells (DC), and tumor associated macrophages (TAM) in groups treated with the gemcitabine-hydrogel complex (Fig. 15A). Moreover, PD-1 expression in  $CD4^+$  and  $CD8^+$  tumor-infiltrating

lymphocytes was enhanced in groups treated with the gemcitabine-hydrogel complex (Fig. 14A). Circulating T-helper type-I cytokines IL-6 and IFN- $\gamma$  also increased after treatment with the gemcitabine-hydrogel complex (Fig. 15B). These results indicate that the ROS-sensitive TSPBA-PVA-gemcitabine complex promotes PD-L1 expression in B16F10 cells, making them identifiable by specific antibodies used in cancer immunotherapy. The underlying mechanism suggests that PD-L1 produced by cancer cells can bind to PD-1 of T-lymphocytic cells, causing immunosuppression and blockage of  $CD4^+$  and  $CD8^+$  production, followed by the inactivation of antigen presenting cells (APCs) (Fig. 15C).<sup>378</sup> Therefore, ROS-responsive hydrogels play a role in promoting immunogenic cancer cell PD-L1 expression, followed by blockage with specific antibodies, representing a promising immunotherapeutic strategy for cancer.<sup>379</sup>

Cold tumors are immunologically inactive, and treatment with a combination of immune checkpoint blockade (ICB) and photodynamic therapies can enhance their elimination.<sup>380,381</sup> However, the photo generated ROS produced by photodynamic therapy can damage immune checkpoint blockade drugs (antibodies), resulting in reduced treatment efficacy.<sup>382</sup> To address this, Zhang *et al.* and Al *et al.* recently reported the synthesis of a Raman-traceable ROS scavenger hydrogel capable of protecting and delivering ICB drugs during photodynamic-ICB combination therapy in T41 tumor-bearing mouse models.<sup>383</sup> The hydrogel was composed of a poly(deca-4,6-diynedioic acid) (PDDA) backbone cross-linked with the natural polysaccharide pullulan. The PDDA-pullulan hydrogel was successfully loaded and co-delivered with a photo inducer (Chlorin e6) and ICB antibody (CD47) for the enhanced killing of T41 tumors. Furthermore, the PDDA-pullulan hydrogel improved the effectiveness of the treatment by prolonging the protection of CD47 from tumor microenvironment-induced ROS, followed by its post-delivery degradation into succinic acid. Both studies mentioned in this section indicate that ROS-responsive hydrogels are promising for co-delivering drugs for anti-cancer treatment.

In addition to delivering chemo-immunotherapy drugs and immune-photodynamic drugs, ROS-sensitive smart hydrogels and nano-carriers have proven effective in delivering a combination of chemo and photodynamic drugs in preclinical mice models.<sup>384,385</sup> In the realm of photodynamic therapy, high-energy radiation triggers the production of reactive oxygen species (ROS), inflicting DNA damage upon the specific cancer cells being targeted.<sup>386</sup> The ingenuity lies in combining this ROS-generating principle with radiation therapy, utilizing nanomaterials that are sensitive to ROS for drug encapsulation. This strategy allows the radiation-induced ROS, besides damaging the DNA of cancer cells, to serve a dual purpose by facilitating the controlled release of encapsulated drugs.<sup>384</sup> This innovative approach not only exploits the synergistic effects of radiation-induced ROS but also significantly amplifies the therapeutic potential of the treatment. Saji Uthaman *et al.* ingeniously fabricated photoactivatable nano-micelles through the self-assembly of a PEG-streamline conjugate (PTS) linked with a reactive oxygen species (ROS)-sensitive



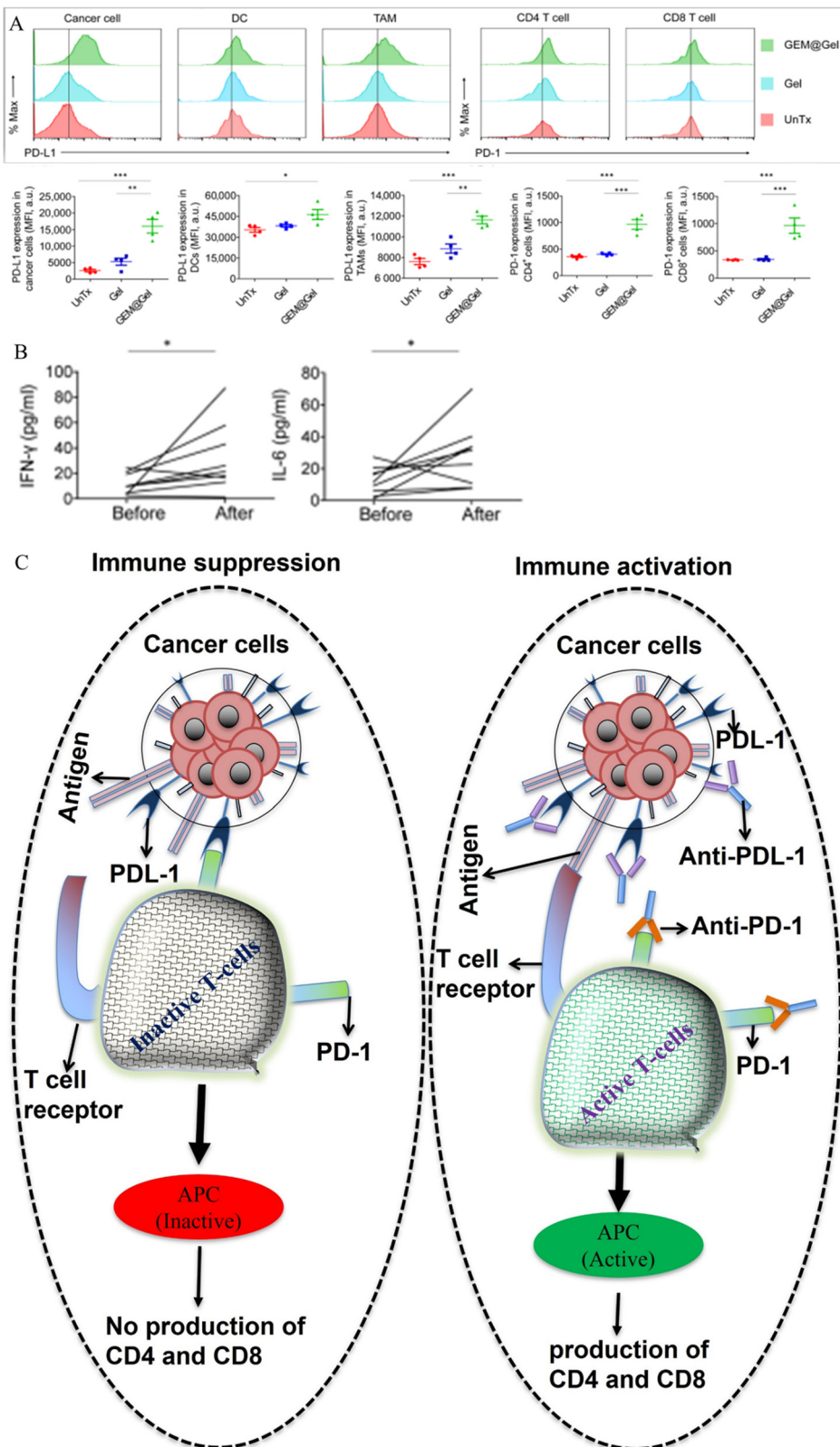


**Fig. 15** (A) Expression of PD-L1 and PD-1 in cancer cells, dendritic cells (DC), tumor-associated macrophages (TAM), CD8<sup>+</sup> T-cells, and CD4<sup>+</sup> T-cells before and after treatment with TSPBA-PVA hydrogel and TSPBA-PVA-gemcitabine complex. Red picks indicate untreated groups, light blue/deep blue picks represent TSPBA gel-treated groups, and green picks denote TSPBA gemcitabine-treated groups. (B) Amount of type I T-helper cytokines, IL-6 and IFN- $\gamma$ , before and after treatment with TSPBA-PVA-gemcitabine complex. (C) Mechanism of T-cell activation and inactivation associated with the PD-L1/PD-1 cascade. Fig. 14A and B, adapted from ref. 377.

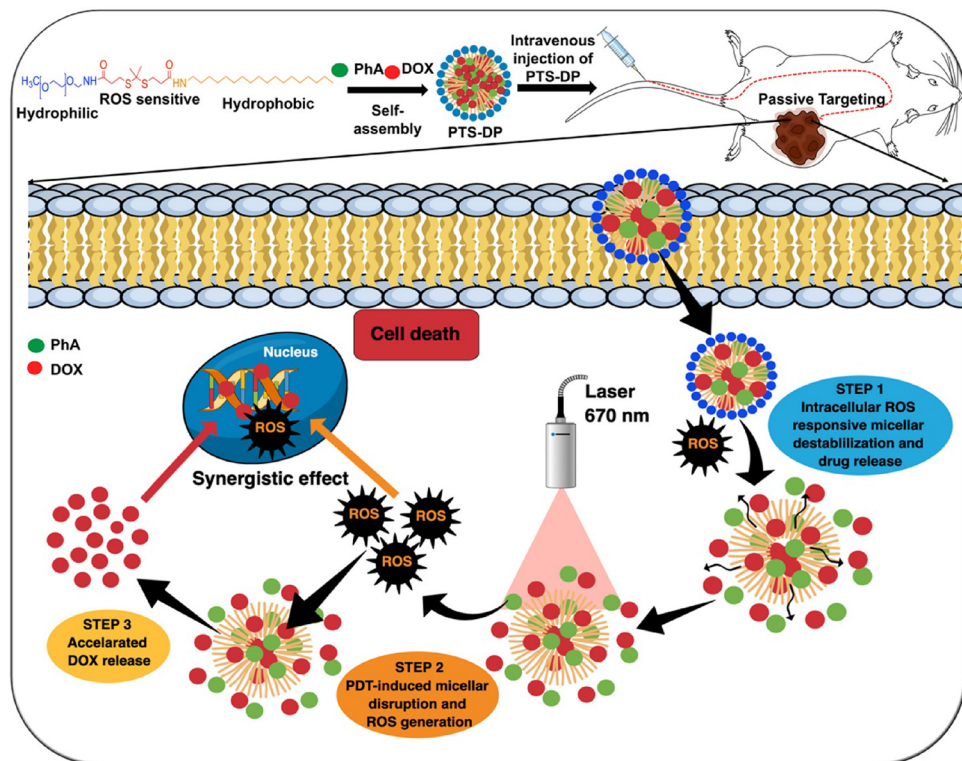


Fig. 16 Schematic illustration of ROS-responsive drug release of PTS-Dox-PhA for enhanced loco regional chemo-photodynamic therapy. Reprinted from ref. 387 with permission of the published (License no. 5651680086971, 17 October 2023).

thioketal linker. This nano-micelle was designed to encapsulate both the chemotherapeutic drug doxorubicin (Dox) and the photosensitizer pheophorbide A (PhA). Sequential release of Dox and PhA was achieved by hydrolyzing the thioketal linker in response to the elevated ROS levels within the tumor microenvironment.<sup>387</sup> Administering these co-drug-loaded PTS nano-micelles *via* intravenous injection in a mouse model of cancer demonstrated their remarkable potential. Once the nano micelles traversed the cell membrane of cancer cells, exposure to the heightened ROS environment within these cells triggered the controlled release of Dox. Subsequently, the application of laser light at 670 nm induced the sequential release of PhA, resulting in a synergistic and controlled therapeutic response (Fig. 16).

## 6. Clinical experiments and application of hydrogels as anti-cancer drug carriers

Clinical application of hydrogels for anti-cancer drug delivery is at an initial stage, number of accredited organizations such as food and drug administration (FDA) approved natural and synthetic-based hydrogels is few in comparison with the pre-clinical approved products.<sup>388</sup> Therefore, even if the application of hydrogels for anti-cancer drug delivery in clinical settings holds significant promise, it also faces several challenges and hurdles in comparison with preclinical settings. Some of the

challenges include; (1) the immune response in preclinical models can exhibit distinct characteristics compared to its manifestation in human clinical trials, potentially resulting in heightened immunogenicity.<sup>389</sup> (2) When implementing hydrogels targeting tumor-specific receptors or proteins for anti-cancer drug delivery in clinical trials, the genetically translated domains of the targeted receptors may present variations compared to preclinical models.<sup>390</sup> (3) The journey from preclinical trials to clinical trials and subsequent regulatory approvals entails rigorous clinical testing, adhering to regulatory standards, and securing FDA authorization, a process known for its time-consuming and resource-intensive nature.<sup>391</sup> (4) Hydrogel-based drug delivery systems, when contrasted with their preclinical counterparts, often incur higher development and manufacturing costs. The challenge lies in scaling up production while ensuring consistent quality.<sup>392</sup> (5) Patient responses to hydrogel-based drug delivery systems can exhibit variability due to factors like individual metabolism, immune responses, and tumor heterogeneity.<sup>393</sup> This may necessitate early adoption of personalized medicine approaches, which can pose initial challenges for funders to embrace. (6) The approval of a hydrogel product in preclinical stages may lead to the emergence of mutated cancer types when applied to humans in a clinical setting.<sup>394</sup>

Among the numerous challenges mentioned, it is noteworthy that both the FDA and EMA (European Medicines Agency) have approved 30 distinct injectable hydrogel products, each intended for various clinical applications. Interestingly, only two of these hydrogels have gained approval specifically for their application in cancer treatment (Table 4).<sup>395</sup>



## 7. Conclusion and research outlook

Local or targeted cancer treatment is emerging as an effective mechanism for minimizing cytotoxicity. Local treatment options have been successfully realized due to the application of hydrogels for the prolonged release of anti-cancer drugs. These carrier hydrogels have attracted increasing attention owing to their low biotoxicity, biodegradability, and stimuli-responsive capacity for delivering anti-cancer drugs.

Thermally sensitive and reactive-species-sensitive hydrogels have recently been used to deliver most anti-cancer drugs in preclinical studies. Copolymer hydrogels composed of PNIPAM, Pluronic, and PEG are thermally sensitive and undergo sol–gel transitions when the temperature changes. After loading anti-cancer drugs into the solution phase, they form a gel when injected into the body and release the incorporated drug at their LCST or UCST for a prolonged time. This mechanism enhances the efficacy of anti-cancer drugs by minimizing toxicity.

ROS-responsive hydrogels are also gaining attention for anti-cancer drug delivery applications. As the tumor microenvironment has an increased amount of ROS, ROS-sensitive hydrogels carry and release drugs to the tumor site in a controlled manner, thereby improving therapeutic outcomes and reducing systemic toxicity. Copolymers composed of Se, Te, aryl boronic esters, poly(L-methionine), poly(L-proline), and disulfides exhibit ROS-responsive properties.

With the increasing need for stimuli-responsive hydrogels, future anti-cancer clinical practice will improve by incorporating the implementation of thermal and ROS-responsive hydrogels for designing multiple deliveries of anti-cancer drugs to achieve successful treatment outcomes.

Based on the level of knowledge that we reached, we recommend the following for future researchers who need to study this area:

- While planning to produce synthetic hydrogels for anti-cancer drug delivery, minimizing cytotoxicity and enhancing long-term drug release is mandatory.
- Since PNIPAM alone has significantly less stability, blending it with stronger copolymers is better.
- Pluronic alone can use as an anti-cancer drug carrier hydrogel. However, its rate of degradation is the fastest. So, we recommend blending it with copolymers having better resistance to degradation.
- PEG and PEG-based hydrogels have innovative stability and biodegradability. Combining PEG with less biodegradable polymers can enhance their biodegradability.
- ROS-responsive hydrogels are at the infant stage and need further research. We believe reducing cytotoxicity is a front-line purpose while synthesizing these hydrogels. We recommend blending the ROS-sensitive group with copolymers having the capacity to minimize toxicity.

## Conflicts of interest

The authors declare no conflict of interest.

Table 4 FDA or EMA approved injectable hydrogels for clinical applications in anti cancer drug delivery

Name (company)	Hydrogel material/payload (gelation mechanism)	Injection type	Approved indication	Approval (year)
SpaceOAR <sup>®</sup> Hydrogel (Augmenix, Inc.)	Polyethylene glycol (chemical reaction)	Percutaneous	To safeguard delicate tissues during radiation therapy for prostate cancer	EMA (2010)
Vantas <sup>®</sup> (Endo pharmaceuticals)	Histrelin acetate, poly(2-hydroxyethyl methacrylate), poly(2-hydroxypropyl methacrylate) and gonadotropin releasing hormone (chemical reaction)	Subcutaneous	Palliative treatment of prostate cancer	FDA (2015) FDA (2004) EMA (2005)



## Acknowledgements

This work was supported by the Ministry of Science and Technology, Taiwan (MOST 109-2221-E-011-146-MY3, 108-2221-E-011-110-MY3 and 108-2923-e-011-005-my3).

## References

- Y. W. Ahmed, *et al.*, *Clin. Epigenet.*, 2022, **14**(1), 1.
- P. Boyle and B. Levin, *World cancer report 2008*, IARC Press, International Agency for Research on Cancer, 2008.
- F. Bray, *et al.*, *Ca-Cancer J. Clin.*, 2018, **68**(6), 394.
- J. Ferlay, *et al.*, *Int. J. Cancer*, 2015, **136**(5), E359.
- C. Mattiuzzi and G. Lippi, *J. Epidemiol. Glob. Health*, 2019, **9**(4), 217.
- S. Senapati, *et al.*, *Signal Transduction Targeted Ther.*, 2018, **3**(1), 7.
- C. Xia, *et al.*, *Chin. Med. J.*, 2022, **135**(5), 584.
- R. F. Barth, *et al.*, *Cancer Commun.*, 2018, **38**(1), 36.
- F. M. Johnston and M. Beckman, *Curr. Oncol. Rep.*, 2019, **21**(8), 67.
- A. Ku, *et al.*, *EJNMMI Radiopharm. Chem.*, 2019, **4**(1), 27.
- S. Rottenberg, *et al.*, *Nat. Rev. Cancer*, 2021, **21**(1), 37.
- J. C. Coffey, *et al.*, *Lancet Oncol.*, 2003, **4**(12), 760.
- L. Wyld, *et al.*, *Nat. Rev. Clin. Oncol.*, 2015, **12**(2), 115.
- W. D. Joo, *et al.*, *Maturitas*, 2013, **76**(4), 308.
- C. Y. Zhao, *et al.*, *Molecules*, 2018, **23**(4), 826.
- D. Schaeue and W. H. McBride, *Nat. Rev. Clin. Oncol.*, 2015, **12**(9), 527.
- J. Thariat, *et al.*, *Nat. Rev. Clin. Oncol.*, 2013, **10**(1), 52.
- L. A. Emens, *et al.*, *Eur. J. Cancer*, 2017, **81**, 116.
- C. L. Ventola, *P T*, 2017, **42**(6), 375.
- N. Shreyash, *et al.*, *ACS Appl. Bio Mater.*, 2021, **4**(3), 2307.
- S. Uthaman, *et al.*, *Biomater. Res.*, 2018, **22**(1), 22.
- C. Roma-Rodrigues, *et al.*, *Pharmaceutics*, 2020, **12**(3), 233.
- C. C. Ma, *et al.*, *Biotechnol. Adv.*, 2020, **40**, 107502.
- D. Liu, *et al.*, *Theranostics*, 2016, **6**(9), 1306.
- V. K. Devi, *et al.*, *Pharmacogn. Rev.*, 2010, **4**(7), 27.
- P. Kumari, *et al.*, *J. Drug Target.*, 2016, **24**(3), 179.
- W. Liu, *et al.*, *Sci. Rep.*, 2021, **11**(1), 199.
- K. Elkhoury, *et al.*, *Pharmaceutics*, 2020, **12**(9), 849.
- S. Huang, *et al.*, *Bioeng. Transl. Med.*, 2022, **7**(3), e10315.
- K. Panduranga Rao, *J. Biomater. Sci., Polym. Ed.*, 1996, **7**(7), 623.
- M. Norouzi, *et al.*, *Drug Discovery Today*, 2016, **21**(11), 1835.
- M. Aquib, *et al.*, *J. Mater. Chem. B*, 2020, **8**(37), 8507.
- Z. Sun, *et al.*, *Mol. Pharm.*, 2019, **17**(2), 373.
- B. Taghizadeh, *et al.*, *Drug Delivery*, 2015, **22**(2), 145.
- M. Sepantafar, *et al.*, *Trends Biotechnol.*, 2017, **35**(11), 1074.
- Q. He, *et al.*, *Asian J. Pharm. Sci.*, 2020, **15**(4), 416.
- Z. K. Huang, *et al.*, *Matter*, 2021, **4**(2), 461.
- H. Xiong, *et al.*, *Small*, 2022, **18**(4), e2104341.
- F. Danhier, *et al.*, *J. Controlled Release*, 2010, **148**(2), 135.
- T. Frenz, *et al.*, *Eur. J. Pharm. Biopharm.*, 2015, **95**(Pt A), 13.
- J. Ghitman, *et al.*, *Mater. Design.*, 2020, **193**, 108805.
- S. Laurent, *et al.*, *Expert Opin. Drug Delivery*, 2014, **11**(9), 1449.
- J. M. Korde and B. Kandasubramanian, *Chem. Eng. J.*, 2020, **379**, 122430.
- Q. V. Nguyen, *et al.*, *Eur. Polym. J.*, 2015, **72**, 602.
- P. Gupta, *et al.*, *Drug Discovery Today*, 2002, **7**(10), 569.
- A. Matsumoto, *et al.*, *Biomacromolecules*, 2003, **4**(5), 1410.
- C. Peng, *et al.*, *J. Controlled Release*, 2022, **345**, 625.
- J. Li and D. J. Mooney, *Nat. Rev. Mater.*, 2016, **1**(12), 1.
- A. Chyzy, *et al.*, *Materials*, 2020, **13**(1), 188.
- E. Caló and V. V. Khutoryanskiy, *Eur. Polym. J.*, 2015, **65**, 252.
- J. Kopeček and J. Yang, *Polym. Int.*, 2007, **56**(9), 1078.
- M. W. Tibbitt and K. S. Anseth, *Biotechnol. Bioeng.*, 2009, **103**(4), 655.
- Q. Chai, *et al.*, *Gels*, 2017, **3**(1), 6.
- A. M. Jonker, *et al.*, *Chem. Mater.*, 2012, **24**(5), 759.
- M. Mahinroosta, *et al.*, *Mater. Today Chem.*, 2018, **8**, 42.
- N. A. Peppas, *et al.*, *Eur. J. Pharm. Biopharm.*, 2000, **50**(1), 27.
- Y. Zhao, *et al.*, *Polymer*, 2005, **46**(14), 5368.
- Y. Zhou, *et al.*, *Carbohydr. Polym.*, 2013, **97**(2), 429.
- A. H. Karoyo and L. D. Wilson, *Materials*, 2021, **14**(5), 1095.
- A. Bashari, *et al.*, *Polym. Adv. Technol.*, 2018, **29**(12), 2853.
- H. R. Culver, *et al.*, *Acc. Chem. Res.*, 2017, **50**(2), 170.
- E. C. Cho, *et al.*, *Macromolecules*, 2003, **36**(26), 9929.
- B. Kaczmarek, *et al.*, *Hydrogels Based Nat. Polym.*, 2020, **151**.
- I. Gibas and H. Janik, *Chem. Chem. Technol.*, 2010, **4**(4), 297.
- F. Ullah, *et al.*, *Mater. Sci. Eng., C*, 2015, **57**, 414.
- T. Vermonden, *et al.*, *Chem. Rev.*, 2012, **112**(5), 2853.
- D. Buenger, *et al.*, *Prog. Polym. Sci.*, 2012, **37**(12), 1678.
- R. Wakabayashi, *et al.*, *Polym. J.*, 2020, **52**(8), 899.
- W. Deng, *et al.*, *Drug Delivery*, 2022, **29**(1), 399.
- F. Khan, *et al.*, *J. Mater. Chem. B*, 2022, **10**(2), 170.
- Y. Tang, *et al.*, *Expert Opin. Drug Delivery*, 2011, **8**(9), 1141.
- W. Hu, *et al.*, *Biomater. Sci.*, 2019, **7**(3), 843.
- J. Q. Zhu, *et al.*, *Adv. Mater.*, 2022, **34**(38), e2201651.
- F. Zhao, *et al.*, *Nanomaterials*, 2015, **5**(4), 2054.
- D. Schmaljohann, *Adv. Drug Delivery Rev.*, 2006, **58**(15), 1655.
- S. Maya, *et al.*, *Curr. Pharm. Des.*, 2013, **19**(41), 7203.
- J. George, *et al.*, *Biotechnol. Adv.*, 2020, **42**, 107370.
- K. Y. Lee and D. J. Mooney, *Chem. Rev.*, 2001, **101**(7), 1869.
- K. T. Nguyen and J. L. West, *Biomaterials*, 2002, **23**(22), 4307.
- J. L. Drury and D. J. Mooney, *Biomaterials*, 2003, **24**(24), 4337.
- X. Wang, *et al.*, *Polymers*, 2017, **9**(9), 401.
- L. R. Nih, *et al.*, *Curr. Opin. Biotechnol.*, 2016, **40**, 155.
- R. A. Stile and K. E. Healy, *Biomacromolecules*, 2001, **2**(1), 185.
- N. A. Peppas, *Biomedical applications of hydrogels handbook*, Springer Science & Business Media, 2010.
- T. D. Sargeant, *et al.*, *Acta Biomater.*, 2012, **8**(1), 124.



- 86 E. A. Kamoun, *et al.*, *Arab. J. Chem.*, 2015, **8**(1), 1.
- 87 Y. Liang, *et al.*, *ACS Nano*, 2021, **15**(8), 12687.
- 88 M. T. Khorasani, *et al.*, *Int. J. Biol. Macromol.*, 2018, **114**, 1203.
- 89 A. Fakhari and C. Berkland, *Acta Biomater.*, 2013, **9**(7), 7081.
- 90 P. Corkhill, *et al.*, *Proc. Inst. Mech. Eng., Part C*, 1990, **204**(3), 147.
- 91 P. C. Nicolson and J. Vogt, *Biomaterials*, 2001, **22**(24), 3273.
- 92 N. Annabi, *et al.*, *Adv. Mater.*, 2014, **26**(1), 85.
- 93 E. Hoch, *et al.*, *Eur. J. Cardiothorac. Surg.*, 2014, **46**(5), 767.
- 94 J. Deng, *et al.*, *Polym. Chem.*, 2017, **8**(14), 2266.
- 95 H. F. Darge, *et al.*, *Int. J. Biol. Macromol.*, 2019, **133**, 545.
- 96 E. M. Ahmed, *J. Adv. Res.*, 2015, **6**(2), 105.
- 97 M. M. Khansari, *et al.*, *Jom*, 2017, **69**(8), 1340.
- 98 S. H. Aswathy, *et al.*, *Helijon*, 2020, **6**(4), e03719.
- 99 C. H. Xian, *et al.*, *Chin. Chem. Lett.*, 2020, **31**(1), 19.
- 100 K. Saini, *PharmaTutor*, 2017, **5**(1), 27.
- 101 J. Hoque, *et al.*, *Macromol. Biosci.*, 2019, **19**(1), e1800259.
- 102 A. da Silva Morais, *et al.*, *Adv. Healthcare Mater.*, 2020, **9**(5), e1901435.
- 103 L. Altomare, *et al.*, *Int. J. Artif. Organs*, 2018, **41**(6), 337.
- 104 C. D. Spicer, *Polym. Chem.*, 2020, **11**(2), 184.
- 105 A. Asti and L. Gioglio, *Int. J. Artif. Organs*, 2014, **37**(3), 187.
- 106 R. Song, *et al.*, *Drug Des., Dev. Ther.*, 2018, **12**, 3117.
- 107 E. Chiellini, *et al.*, *Prog. Polym. Sci.*, 2003, **28**(6), 963.
- 108 S. Tabasum, *et al.*, *Int. J. Biol. Macromol.*, 2018, **120**(Pt A), 603.
- 109 R. A. Abd Alsaheb, *et al.*, *J. Chem. Pharm. Res.*, 2015, **7**(12), 51.
- 110 A. D. Lynn, *et al.*, *J. Biomed. Mater. Res., Part A*, 2010, **93**(3), 941.
- 111 D. Selktar, *Science*, 2012, **336**(6085), 1124.
- 112 D. F. Al Husaeni and A. B. D. Nandyanto, *ASEAN J. Sci. Eng.*, 2022, **2**(1), 19.
- 113 N. J. van Eck and L. Waltman, *Scientometrics*, 2017, **111**(2), 1053.
- 114 B. George, *et al.*, *Eur. Polym. J.*, 2021, **157**, 110640.
- 115 C. Biscaro and C. Giupponi, *PLoS One*, 2014, **9**(6), e99502.
- 116 F. Andrade, *et al.*, *Cancers*, 2021, **13**(5), 1164.
- 117 C. C. Lin and K. S. Anseth, *Pharm. Res.*, 2009, **26**(3), 631.
- 118 R. Dimatteo, *et al.*, *Adv. Drug Delivery Rev.*, 2018, **127**, 167.
- 119 J. Omar, *et al.*, *Chem. – Asian J.*, 2022, **17**(9), e202200081.
- 120 A. Pourjavadi, *et al.*, *New J. Chem.*, 2021, **45**(35), 15705.
- 121 G. Saravanakumar, *et al.*, *Adv. Sci.*, 2017, **4**(1), 1600124.
- 122 K. S. Soppimath, *et al.*, *Drug. Dev. Ind. Pharm.*, 2002, **28**(8), 957.
- 123 A. Kasiński, *et al.*, *Int. J. Nanomed.*, 2020, **15**, 4541.
- 124 A. K. Bajpai, *et al.*, *Prog. Polym. Sci.*, 2008, **33**(11), 1088.
- 125 M. A. H. Badsha, *et al.*, *J. Hazard Mater.*, 2021, **408**, 124463.
- 126 J. F. Mano, *Adv. Eng. Mater.*, 2008, **10**(6), 515.
- 127 E. S. Gil and S. M. Hudson, *Prog. Polym. Sci.*, 2004, **29**(12), 1173.
- 128 J. H. Lee, *Biomater. Res.*, 2018, **22**(1), 27.
- 129 L. J. Chen and H. B. Yang, *Acc. Chem. Res.*, 2018, **51**(11), 2699.
- 130 M. A. Stuart, *et al.*, *Nat. Mater.*, 2010, **9**(2), 101.
- 131 C. de Las Heras Alarcon, *et al.*, *Chem. Soc. Rev.*, 2005, **34**(3), 276.
- 132 B. Guo, *et al.*, *J. Am. Chem. Soc.*, 2020, **142**(41), 17318.
- 133 J. Hu, *et al.*, *J. Polym. Res.*, 2012, **19**(11), 1.
- 134 H. Gupta, *et al.*, *Drug Delivery*, 2007, **14**(8), 507.
- 135 T. M. Aminabhavi, *et al.*, *J. Appl. Polym. Sci.*, 2004, **94**(5), 2057.
- 136 L. L. Li, *et al.*, *J. Appl. Polym. Sci.*, 2012, **124**(2), 1128.
- 137 S. J. Buwalda, *et al.*, *J. Controlled Release*, 2014, **190**, 254.
- 138 M. R. Matanović, *et al.*, *Int. J. Pharm.*, 2014, **472**(1–2), 262.
- 139 S. Wong, *et al.*, *J. Mater. Chem. B*, 2014, **2**(6), 595.
- 140 Y. Kaneko, *et al.*, *J. Membr. Sci.*, 1995, **101**(1–2), 13.
- 141 F. M. Goycoolea, *et al.*, *Polym. Bull.*, 2007, **58**(1), 225.
- 142 M. Constantin, *et al.*, *Express Polym. Lett.*, 2011, **5**(10), 839.
- 143 Y. Chen, *et al.*, *Sci. Rep.*, 2016, **6**(1), 31593.
- 144 L. Klouda and A. G. Mikos, *Eur. J. Pharm. Biopharm.*, 2008, **68**(1), 34.
- 145 H. Huang, *et al.*, *Saudi Pharm. J.*, 2019, **27**(7), 990.
- 146 E. Ruel-Gariepy and J. C. Leroux, *Eur. J. Pharm. Biopharm.*, 2004, **58**(2), 409.
- 147 Y. Kotsuchibashi, *Polym. J.*, 2020, **52**(7), 681.
- 148 Y. J. Kim and Y. T. Matsunaga, *J. Mater. Chem. B*, 2017, **5**(23), 4307.
- 149 J. Seuring and S. Agarwal, *Macromol. Rapid Commun.*, 2012, **33**(22), 1898.
- 150 Y. Huang, *et al.*, *RSC Adv.*, 2017, **7**(46), 28711.
- 151 Y. L. Ding, *et al.*, *ACS Appl. Polym. Mater.*, 2020, **2**(8), 3259.
- 152 M. Najafi, *et al.*, *Soft Matter*, 2021, **17**(8), 2132.
- 153 Y. Biswas, *et al.*, *Polym. Chem.*, 2016, **7**(4), 867.
- 154 M. Sponchioni, *et al.*, *Mater. Sci. Eng., C*, 2019, **102**, 589.
- 155 J. A. McCune, *et al.*, *Adv. Mater.*, 2020, **32**(20), e1906890.
- 156 M. J. Taylor, *et al.*, *Gels*, 2017, **3**(1), 4.
- 157 S. Zhuo, *et al.*, *Polymers*, 2022, **14**(15), 3155.
- 158 A. Gandhi, *et al.*, *Asian J. Pharm. Sci.*, 2015, **10**(2), 99.
- 159 J. Omar, *et al.*, *Chem. – Asian J.*, 2022, **17**(9), e202200081.
- 160 J. Maitra and V. K. Shukla, *Am. J. Polym. Sci.*, 2014, **4**(2), 25.
- 161 U. S. Madduma-Bandarage and S. V. Madihally, *J. Appl. Polym. Sci.*, 2021, **138**(19), 50376.
- 162 S. G. Roy and P. De, *Polymer*, 2014, **55**(21), 5425.
- 163 E. M. Ahmed, *J. Adv. Res.*, 2015, **6**(2), 105.
- 164 S. H. Zainal, *et al.*, *J. Mater. Res. Technol.*, 2021, **10**, 935.
- 165 A. Pourjavadi, *et al.*, *Eur. Polym. J.*, 2004, **40**(7), 1363.
- 166 K. Vats, *et al.*, *J. Biomed. Mater. Res., Part A*, 2017, **105**(4), 1112.
- 167 M. M. Elsayed, *J. Polym. Environ.*, 2019, **27**(4), 871.
- 168 Y. Gao, *et al.*, *Adv. Mater.*, 2021, **33**(25), 2006362.
- 169 H. Mittal, *et al.*, *Macromol. Mater. Eng.*, 2016, **301**(5), 496.
- 170 D. Rana, *et al.*, *Gels*, 2023, **9**(8), 643.
- 171 P. Matricardi, *et al.*, *Adv. Drug Delivery Rev.*, 2013, **65**(9), 1172.
- 172 M. Rahimi and M. Nasiri, *Eur. Polym. J.*, 2020, **125**, 109536.
- 173 A. Saeed, *et al.*, *React. Funct. Polym.*, 2010, **70**(4), 230.
- 174 Y. Xiao, *et al.*, *Colloids Surf. B*, 2021, **200**, 111581.
- 175 Z. J. Wang, *et al.*, *J. Cleaner Prod.*, 2018, **176**, 1292.
- 176 A. Kumar, *et al.*, *Prog. Polym. Sci.*, 2007, **32**(10), 1205.



- 177 B. Strachota, *et al.*, *J. Mater. Res. Technol.*, 2021, **15**, 6079.
- 178 L. Liang, *et al.*, *Langmuir*, 2000, **16**(21), 8016.
- 179 A. Aghabegi Moghanjoughi, *et al.*, *Drug Delivery Transl. Res.*, 2016, **6**(3), 333.
- 180 C. Tsitsilianis, *Soft Matter*, 2010, **6**(11), 2372.
- 181 M. Karimi, *et al.*, *ACS Appl. Mater. Interfaces*, 2016, **8**(33), 21107.
- 182 D. J. Overstreet, *et al.*, *Soft Mater.*, 2013, **11**(3), 294.
- 183 R. X. Liu, *et al.*, *Colloid Polym. Sci.*, 2009, **287**(6), 627.
- 184 M. J. Ansari, *et al.*, *Gels*, 2022, **8**(7), 454.
- 185 H. A. Nair *et al.*, Stimuli-responsive micelles: a nanoplateform for therapeutic and diagnostic applications, *Drug Targeting and Stimuli Sensitive Drug Delivery Systems*, Elsevier, 2018, pp. 303.
- 186 F. Doberenz, *et al.*, *J. Mater. Chem. B*, 2020, **8**(4), 607.
- 187 L.-W. Xia, *et al.*, *Nat. Commun.*, 2013, **4**(1), 2226.
- 188 Y. Yang, *et al.*, *View*, 2021, **2**(2), 20200042.
- 189 A. S. Patil, *et al.*, *Top. Catal.*, 2022, **65**(19–20), 2005.
- 190 J. Ma, *et al.*, *Drug Delivery*, 2022, **29**(1), 1457.
- 191 E. Askari, *et al.*, *Gels*, 2020, **6**(2), 14.
- 192 D. Lin, *et al.*, *Macromol. Biosci.*, 2019, **19**(6), e1900001.
- 193 H. Qiu, *et al.*, *Trends Biotechnol.*, 2020, **38**(6), 579.
- 194 Y. Li, *et al.*, *Chem. Rev.*, 2015, **115**(16), 8564.
- 195 S. M. Cuya, *et al.*, *Cancer Chemother. Pharmacol.*, 2017, **80**(1), 1.
- 196 G. Capranico, *et al.*, *J. Med. Chem.*, 2017, **60**(6), 2169.
- 197 A. A. Alghorabi, *et al.*, *J. Cancer Res.*, 2019, **7**, 17.
- 198 E. I. Vrettos, *et al.*, *Beilstein J. Org. Chem.*, 2018, **14**(1), 930.
- 199 A. Pourjavadi, *et al.*, *New J. Chem.*, 2020, **44**(40), 17302.
- 200 S. Havanur, *et al.*, *Mater. Sci. Eng., C*, 2019, **105**, 110094.
- 201 Y. Yang, *et al.*, *J. Controlled Release*, 2009, **135**(2), 175.
- 202 S. Khan, *et al.*, *AAPS PharmSciTech*, 2019, **20**(3), 119.
- 203 H. Bera, *et al.*, *Mater. Sci. Eng., C*, 2020, **110**, 110628.
- 204 C. Gomez, *et al.*, *J. Microencapsul.*, 2012, **29**(7), 626.
- 205 F. Andrade, *et al.*, *Carbohydr. Polym.*, 2022, **295**, 119859.
- 206 M. Fathi, *et al.*, *Int. J. Biol. Macromol.*, 2019, **128**, 957.
- 207 F. Salimi, *et al.*, *Artif. Cells, Nanomed., Biotechnol.*, 2018, **46**(5), 949.
- 208 R. P. Johnson, *et al.*, *Biomacromolecules*, 2013, **14**(5), 1434.
- 209 C. Cheng, *et al.*, *J. Mater. Sci.*, 2015, **50**(14), 4914.
- 210 G. Bonacucina, *et al.*, *Polymers*, 2011, **3**(2), 779.
- 211 Le, T. V. Vo, *et al.*, *Int. J. Polym. Anal. Charact.*, 2022, **27**(3), 205.
- 212 M. Gou, *et al.*, *Int. J. Pharm.*, 2008, **359**(1–2), 228.
- 213 Z. He and P. Alexandridis, *Polymers*, 2017, **10**(1), 32.
- 214 S. Peng, *et al.*, *Mater. Sci. Eng., C*, 2016, **69**, 421.
- 215 M. Perez-Page, *et al.*, *Adv. Colloid Interface Sci.*, 2016, **234**, 51.
- 216 S. Y. Lee, *et al.*, *Macromol. Chem. Phys.*, 2010, **211**(6), 692.
- 217 P. Alexandridis, *et al.*, *Macromolecules*, 1994, **27**(9), 2414.
- 218 N. J. Jain, *et al.*, *Colloids Surf. A*, 2000, **173**(1–3), 85.
- 219 K. Nakashima and P. Bahadur, *Adv. Colloid Interface Sci.*, 2006, **123–126**, 75.
- 220 M. McKenzie, *et al.*, *Molecules*, 2015, **20**(11), 20397.
- 221 X. Guo, *et al.*, *J. Polym. Sci., Polym. Chem.*, 2016, **54**(22), 3525.
- 222 A. V. Kabanov and V. Y. Alakhov, *Crit. Rev. Ther. Drug Carrier Syst.*, 2002, **19**(1), 1.
- 223 A. Naharro-Molinero, *et al.*, *Pharmaceutics*, 2022, **14**(12), 2628.
- 224 A. Hatefi and B. Amsden, *J. Controlled Release*, 2002, **80**(1–3), 9.
- 225 T. Betancourt, *et al.*, *J. Biomed. Mater. Res., Part A*, 2009, **91**(1), 263.
- 226 P. Zarrintaj, *et al.*, *Acta Biomater.*, 2020, **110**, 37.
- 227 R. Parhi, *Adv. Pharm. Bull.*, 2017, **7**(4), 515.
- 228 B. D. Ulery, *et al.*, *J. Polym. Sci., Part B: Polym. Phys.*, 2011, **49**(12), 832.
- 229 J. H. Ryu, *et al.*, *Biomacromolecules*, 2011, **12**(7), 2653.
- 230 Z. Li and J. Guan, *Expert Opin. Drug Delivery*, 2011, **8**(8), 991.
- 231 P. Singla, *et al.*, *Adv. Colloid Interface Sci.*, 2022, **299**, 102563.
- 232 H. J. Yoon and W. D. Jang, *J. Mater. Chem.*, 2010, **20**(2), 211.
- 233 T. Coviello, *et al.*, *J. Controlled Release*, 2007, **119**(1), 5.
- 234 A. Sosnik and K. P. Seremeta, *Gels*, 2017, **3**(3), 25.
- 235 M. Saeedi, *et al.*, *J. Controlled Release*, 2022, **350**, 175.
- 236 H. Abdeltawab, *et al.*, *Expert Opin. Drug Delivery*, 2020, **17**(4), 495.
- 237 M. Salem, *et al.*, *RSC Adv.*, 2014, **4**(21), 10815.
- 238 L. Bromberg, *Expert Opin. Drug Delivery*, 2005, **2**(6), 1003.
- 239 S. Nie, *et al.*, *Int. J. Nanomed.*, 2011, **6**, 151.
- 240 I. Dimitrov, *et al.*, *Prog. Polym. Sci.*, 2007, **32**(11), 1275.
- 241 B. Sun, *et al.*, *Curr. Med. Chem.*, 2019, **26**(14), 2485.
- 242 C. Y. Ting, *et al.*, *Biomaterials*, 2012, **33**(2), 704.
- 243 K. Mitusova, *et al.*, *J. Nanobiotechnol.*, 2022, **20**(1), 412.
- 244 L. C. S. Erthal, *et al.*, *Acta Biomater.*, 2021, **121**, 89.
- 245 M. H. Turabee, *et al.*, *Carbohydr. Polym.*, 2019, **203**, 302.
- 246 M. Norouzi, *et al.*, *Int. J. Pharm.*, 2021, **598**, 120316.
- 247 B. de Melo Santana, *et al.*, *Pharmaceutics*, 2022, **14**(12), 2837.
- 248 D. S. Shaker, *et al.*, *J. Drug Delivery Sci. Technol.*, 2016, **35**, 155.
- 249 W. K. Bae, *et al.*, *Biomaterials*, 2013, **34**(4), 1433.
- 250 Q. Wen, *et al.*, *Int. J. Pharm.*, 2020, **582**, 119334.
- 251 H. Sadeghi-Abandansari, *et al.*, *Eur. Polym. J.*, 2021, **157**, 110646.
- 252 M. Kiseleva, *et al.*, *ACS Biomater. Sci. Eng.*, 2022, **8**(3), 1200.
- 253 J. Li, *et al.*, *Int. J. Biol. Macromol.*, 2019, **134**, 63.
- 254 D. Y. Kim, *et al.*, *Biomaterials*, 2016, **85**, 232.
- 255 T. Zambanini, *et al.*, *Materials*, 2021, **14**(6), 1459.
- 256 T. T. Hoang Thi, *et al.*, *Polymers*, 2020, **12**(2), 298.
- 257 P. F. Fuchs, *et al.*, *J. Chem. Theory Comput.*, 2012, **8**(10), 3943.
- 258 H. Ishihara, *Biol. Pharm. Bull.*, 2013, **36**(6), 883.
- 259 H. Akhdar, *et al.*, *Nucl. Eng. Technol.*, 2022, **54**(2), 701.
- 260 J. Li, *et al.*, *Cancer Sci.*, 2018, **109**(6), 1958.
- 261 P. Caliceti and F. M. Veronese, *Adv. Drug Delivery Rev.*, 2003, **55**(10), 1261.
- 262 K. Knop, *et al.*, *Angew. Chem., Int. Ed.*, 2010, **49**(36), 6288.
- 263 B. Tyler, *et al.*, *Adv. Drug Delivery Rev.*, 2016, **107**, 163.
- 264 W. E. Hennink and C. F. van Nostrum, *Adv. Drug Delivery Rev.*, 2012, **64**, 223.
- 265 A. D'Souza A and R. Shegokar, *Expert Opin. Drug Delivery*, 2016, **13**(9), 1257.



- 266 J. A. Barreto, *et al.*, *Adv. Mater.*, 2011, **23**(12), H18.
- 267 N. A. Peppas, *et al.*, *J. Controlled Release*, 1999, **62**(1-2), 81.
- 268 Y. Li, *et al.*, *Chem. Soc. Rev.*, 2012, **41**(6), 2193.
- 269 S. S. Liow, *et al.*, *MRS Bull.*, 2016, **41**(7), 557.
- 270 T. K. Endres, *et al.*, *Biomaterials*, 2011, **32**(30), 7721.
- 271 X. J. Loh, *et al.*, *J. Controlled Release*, 2010, **143**(2), 175.
- 272 H. F. Darge, *et al.*, *Chem. Eng. J.*, 2021, **406**, 126879.
- 273 A. Teotia *et al.*, Thermo-responsive polymers: structure and design of smart materials, *Switchable and responsive surfaces and materials for biomedical applications*, Elsevier, 2015, p. 3.
- 274 K. Nagahama, *et al.*, *Adv. Funct. Mater.*, 2008, **18**(8), 1220.
- 275 J. Shi, *et al.*, *Acta Biomater.*, 2021, **128**, 42.
- 276 I. Gibas and H. Janik, (2010).
- 277 A. Kumari, *et al.*, *Colloids Surf. B*, 2010, **75**(1), 1.
- 278 A. Alexander, *et al.*, *Eur. J. Pharm. Biopharm.*, 2014, **88**(3), 575.
- 279 Q. Yang, *et al.*, *J. Mater. Chem.*, 2011, **21**(9), 2783.
- 280 N. K. Singh and D. S. Lee, *J. Controlled Release*, 2014, **193**, 214.
- 281 P. K. Sharma, *et al.*, *ACS Appl. Mater. Interfaces*, 2018, **10**(37), 30936.
- 282 X. Wu, *et al.*, *Biomaterials*, 2016, **75**, 148.
- 283 X. Sui, *et al.*, *PLoS One*, 2014, **9**(5), e97781.
- 284 S. Ling, *et al.*, *Mol. Med. Rep.*, 2014, **10**(6), 2891.
- 285 A. Paone, *et al.*, *Cell Death Dis.*, 2014, **5**(11), e1525.
- 286 H. F. Darge, *et al.*, *Int. J. Pharm.*, 2019, **572**, 118799.
- 287 P. K. Sharma, *et al.*, *ACS Appl. Mater. Interfaces*, 2018, **10**(37), 30936.
- 288 F. P. Seib, *et al.*, *ACS Biomater. Sci. Eng.*, 2016, **2**(12), 2287.
- 289 C. T. Tsao, *et al.*, *Biomacromolecules*, 2014, **15**(7), 2656.
- 290 A. D. Guerra, *et al.*, *Theranostics*, 2017, **7**(15), 3732.
- 291 S. A. Meenach, *et al.*, *Acta Biomater.*, 2010, **6**(3), 1039.
- 292 V. H. G. Phan, *et al.*, *RSC Adv.*, 2016, **6**(47), 41644.
- 293 B. S. Makhmalzadeh, *et al.*, *J. Pharm. Pharm. Sci.*, 2018, **21**(1), 143.
- 294 M. Si, *et al.*, *Int. J. Nanomed.*, 2022, **17**, 1309.
- 295 V. L. Truong, *et al.*, *Biofactors*, 2018, **44**(1), 36.
- 296 D. A. Wink, *et al.*, *J. Leukoc. Biol.*, 2011, **89**(6), 873.
- 297 H. Xie, *et al.*, *J. Dermatol. Sci.*, 2016, **81**(1), 3.
- 298 L. I. Leichert and U. Jakob, *PLoS Biol.*, 2004, **2**(11), e333.
- 299 I. Hanukoglu, *Drug Metab. Rev.*, 2006, **38**(1-2), 171.
- 300 P. Guerin, *et al.*, *Hum. Reprod. Update*, 2001, **7**(2), 175.
- 301 C. A. Juan, *et al.*, *Int. J. Mol. Sci.*, 2021, **22**(9), 4642.
- 302 Q. Kang and C. Yang, *Redox Biol.*, 2020, **37**, 101799.
- 303 A. H. Bhat, *et al.*, *Biomed. Pharmacother.*, 2015, **74**, 101.
- 304 M. Delfi, *et al.*, *Nano Today*, 2021, **38**, 101119.
- 305 I. Kareva, *Transl. Oncol.*, 2011, **4**(5), 266.
- 306 M. A. Feitelson *et al.*, Sustained proliferation in cancer: Mechanisms and novel therapeutic targets, *Seminars in cancer biology*, Elsevier, 2015, vol. 35, p. S25.
- 307 P. T. Schumacker, *Cancer Cell*, 2006, **10**(3), 175.
- 308 S. Galadari, *et al.*, *Free Radical Biol. Med.*, 2017, **104**, 144.
- 309 R. Li, *et al.*, *React. Oxygen Species*, 2016, **1**(1), 9.
- 310 B. Niu, *et al.*, *Biomaterials*, 2021, **277**, 121110.
- 311 L. L. Policastro, *et al.*, *Antioxid. Redox Signaling*, 2013, **19**(8), 854.
- 312 R. Van Wijk and W. W. Van Solinge, *Blood*, 2005, **106**(13), 4034.
- 313 S. Singh, *et al.*, *Int. J. Plant Physiol. Biochem.*, 2012, **4**(1), 1.
- 314 N. Koju, *et al.*, *Acta Pharm. Sin.*, 2022, **43**(8), 1889.
- 315 H. Y. Tang, *et al.*, *Antioxid. Redox Signaling*, 2015, **22**(9), 744.
- 316 M. Farina and M. Aschner, *Biochim. Biophys. Acta, Gen. Subj.*, 2019, **1863**(12), 129285.
- 317 R. van Zwieten, *et al.*, *Free Radical Biol. Med.*, 2014, **67**, 377.
- 318 C. S. Cho, *et al.*, *Antioxid. Redox Signal*, 2010, **12**(11), 1235.
- 319 M. M. Al-Gayyar, *et al.*, *J. Pharm. Pharmacol.*, 2007, **59**(3), 409.
- 320 H. Pelicano, *et al.*, *Drug Resistance Updates*, 2004, **7**(2), 97.
- 321 J. Song, *et al.*, *Life*, 2022, **12**(2), 271.
- 322 S. Verma, *et al.*, *World J. Biol. Chem.*, 2014, **5**(3), 355.
- 323 C. J. Hsieh, *et al.*, *Free Radical Biol. Med.*, 2014, **67**, 159.
- 324 V. Okoh, *et al.*, *Biochim. Biophys. Acta*, 2011, **1815**(1), 115.
- 325 P. Storz, *Front. Biosci.*, 2005, **10**(2), 1881.
- 326 G. Zhang, *et al.*, *Cell Death Disease*, 2019, **10**(4), 255.
- 327 D. Chen, *et al.*, *Oncol. Rep.*, 2011, **26**(5), 1287.
- 328 A. M. Knaapen, *et al.*, *Int. J. Cancer*, 2004, **109**(6), 799.
- 329 E. Bishop and T. D. Bradshaw, *Cancer Chemother. Pharmacol.*, 2018, **82**(6), 913.
- 330 I. Mfouo-Tynga and H. Abrahamse, *Int. J. Mol. Sci.*, 2015, **16**(5), 10228.
- 331 L. B. Sullivan and N. S. Chandel, *Cancer Metab.*, 2014, **2**, 17.
- 332 G. Y. Liou and P. Storz, *Free Radical Res.*, 2010, **44**(5), 479.
- 333 H. Yang, *et al.*, *J. Exp. Clin. Cancer Res.*, 2018, **37**(1), 266.
- 334 D. Trachootham, *et al.*, *Nat. Rev. Drug Discovery*, 2009, **8**(7), 579.
- 335 Q. Tang, *et al.*, *Curr. Med. Chem.*, 2018, **25**(16), 1837.
- 336 H. S. El-Sawy, *et al.*, *ACS Nano*, 2018, **12**(11), 10636.
- 337 C. Ding, *et al.*, *Molecules*, 2016, **21**(12), 1715.
- 338 H. Ye, *et al.*, *Biomacromolecules*, 2019, **20**(7), 2441.
- 339 C. Tapeinos and A. Pandit, *Adv. Mater.*, 2016, **28**(27), 5553.
- 340 Z. Cao, *et al.*, *Acta Biomater.*, 2021, **130**, 17.
- 341 W. Tao and Z. He, *Asian J. Pharm. Sci.*, 2018, **13**(2), 101.
- 342 F. Gao and Z. Xiong, *Front. Chem.*, 2021, **9**, 649048.
- 343 Y. Teng, *et al.*, *Crit. Rev. Environm. Sci. Technol.*, 2019, **49**(24), 2314.
- 344 S. Shankar, *et al.*, *Crit. Rev. Environm. Sci. Technol.*, 2021, **51**(20), 2329.
- 345 B. D. Fairbanks, *et al.*, *Macromolecules*, 2011, **44**(8), 2444.
- 346 P. Hu and N. Tirelli, *Bioconjugate Chem.*, 2012, **23**(3), 438.
- 347 A. Napoli, *et al.*, *Nat. Mater.*, 2004, **3**(3), 183.
- 348 J. Liang and B. Liu, *Bioeng. Transl. Med.*, 2016, **1**(3), 239.
- 349 S. Aksakal, *et al.*, *Sulfur-Containing Polym.*, 2021, 235.
- 350 M. Criado-Gonzalez and D. Mecerreyes, *J. Mater. Chem. B*, 2022, **10**(37), 7206.
- 351 Z. Zhou, *et al.*, *Angew. Chem., Int. Ed.*, 2018, **57**(28), 8463.
- 352 M. C. Branco and J. P. Schneider, *Acta Biomater.*, 2009, **5**(3), 817.
- 353 J. Zhou, *et al.*, *Smart Mater. Med.*, 2023, DOI: [10.1002/SMMD.20220026](https://doi.org/10.1002/SMMD.20220026).
- 354 M. S. Shim and Y. Xia, *Angew. Chem., Int. Ed.*, 2013, **52**(27), 6926.



- 355 N. Yang, *et al.*, *Nanomicro. Lett.*, 2020, **12**(1), 15.
- 356 N. Ma, *et al.*, *J. Am. Chem. Soc.*, 2010, **132**(2), 442.
- 357 N. Ma, *et al.*, *Polym. Chem.*, 2010, **1**(10), 1609.
- 358 R. R. Ramoutar and J. L. Brumaghim, *Cell Biochem. Biophys.*, 2010, **58**(1), 1.
- 359 F. Maiyo and M. Singh, *Nanomedicine*, 2017, **12**(9), 1075.
- 360 S. H. Lee, *et al.*, *Adv. Healthcare Mater.*, 2013, **2**(6), 908.
- 361 W. Cao, *et al.*, *Angew. Chem., Int. Ed.*, 2013, **52**(24), 6233.
- 362 W. Cao, *et al.*, *Nano Today*, 2015, **10**(6), 717.
- 363 L. Wang, *et al.*, *ACS Appl. Mater. Interfaces*, 2015, **7**(29), 16054.
- 364 F. Li, *et al.*, *Biomaterials*, 2017, **133**, 208.
- 365 S. Obuobi, *et al.*, *Adv. Healthcare Mater.*, 2018, **7**(13), e1701388.
- 366 C. Ruan, *et al.*, *ACS Appl. Mater. Interfaces*, 2018, **10**(12), 10398.
- 367 J. Lu, *et al.*, *ACS Appl. Mater. Interfaces*, 2019, **11**(10), 10337.
- 368 F. El-Mohtadi, *et al.*, *Macromol. Rapid Commun.*, 2019, **40**(1), e1800699.
- 369 Y. Xue, *et al.*, *Chem. Soc. Rev.*, 2021, **50**(8), 4872.
- 370 M. Mazurowski, *et al.*, *Macromolecules*, 2012, **45**(22), 8970.
- 371 C. G. Hardy, *et al.*, *J. Polym. Sci. Pol. Chem.*, 2011, **49**(6), 1409.
- 372 D. Astruc, *Eur. J. Inorg. Chem.*, 2017, (1), 6.
- 373 Y. Na, *et al.*, *J. Mater. Chem. B*, 2020, **8**(9), 1906.
- 374 D. Li, *et al.*, *Adv. Healthcare Mater.*, 2020, **9**(20), e2000605.
- 375 F. Xu, *et al.*, *ACS Appl. Mater. Interfaces*, 2017, **9**(6), 5181.
- 376 J. Tan, *et al.*, *Chem.*, 2019, **5**(7), 1775.
- 377 C. Wang, *et al.*, *Sci. Transl. Med.*, 2018, **10**(429), eaan3682.
- 378 V. Pulko, *et al.*, *J. Immunol.*, 2011, **187**(11), 5606.
- 379 X. Zhang, *et al.*, *Gels*, 2021, **7**(4), 224.
- 380 J. Zang, *et al.*, *Chem. Eng. J.*, 2022, **434**, 134585.
- 381 J. Huang, *et al.*, *Adv. Funct. Mater.*, 2021, **31**(21), 2011171.
- 382 G. M. Cramer, *et al.*, *Photochem. Photobiol.*, 2020, **96**(5), 954.
- 383 Y. Zhang, *et al.*, *Nat. Commun.*, 2022, **13**(1), 4553.
- 384 Z. Cao, *et al.*, *Acta Biomater.*, 2021, **130**, 17.
- 385 F. Danhier, *et al.*, *J. Controlled Release*, 2010, **148**(2), 135.
- 386 D. Chen, *et al.*, *Small*, 2021, **17**(31), 2006742.
- 387 S. Uthaman, *et al.*, *Biomaterials*, 2020, **232**, 119702.
- 388 Q.-q. Wang, *et al.*, *Technol. Cancer Res. Treat.*, 2023, **22**, 15330338221150322.
- 389 D. G. Leach, *et al.*, *Acta Biomater.*, 2019, **88**, 15.
- 390 L. P. Ganipineni, *et al.*, *J. Controlled Release*, 2018, **281**, 42.
- 391 J. I. Hare, *et al.*, *Adv. Drug Delivery Rev.*, 2017, **108**, 25.
- 392 G. Agrawal, *et al.*, *Biotechnol. Prog.*, 2021, **37**(3), e3126.
- 393 M. Sonker, *et al.*, *ACS Appl. Bio Mater.*, 2021, **4**(12), 8080.
- 394 S. Correa, *et al.*, *Chem. Rev.*, 2021, **121**(18), 11385.
- 395 A. Mandal, *et al.*, *Bioeng. Transl. Med.*, 2020, **5**(2), e10158.

